2. THE STUDY OF EQUILIBRIUM STATES BY THE METHODS OF THERMAL ANALYSIS

2.1. General outline

The variables which characterize the state of a system are mutually related in the form of relationships, based on thermodynamics, which permits the choice of convenient, easily measured quantities which facilitate the experimental study of the equilibrium states. The mathematical treatment is then limited to the quantities which are difficult to measure.

When constructing the phase diagram of a binary system by direct investigation of the composition of phases at different temperatures, the calculation of the heat of fusion of individual components is possible. This is an advantage because a direct measurement of the heat of fusion at high temperatures is difficult. On the other hand, it is possible to find the dependence of phase transitions on temperature if an experimental technique is available to determine the heat of fusion and thermodynamic data of solutions (see Table 2.1a). This procedure can also be extended to phase transitions of second order and to chemical reactions (see Table 2.1b).

TABLE 2.1
COMPLEMENTARY WAYS FOR STUDYING (a) PHASE EQUILIBRIA AND (b) EQUILIBRIA IN CHEMICAL REACTIONS

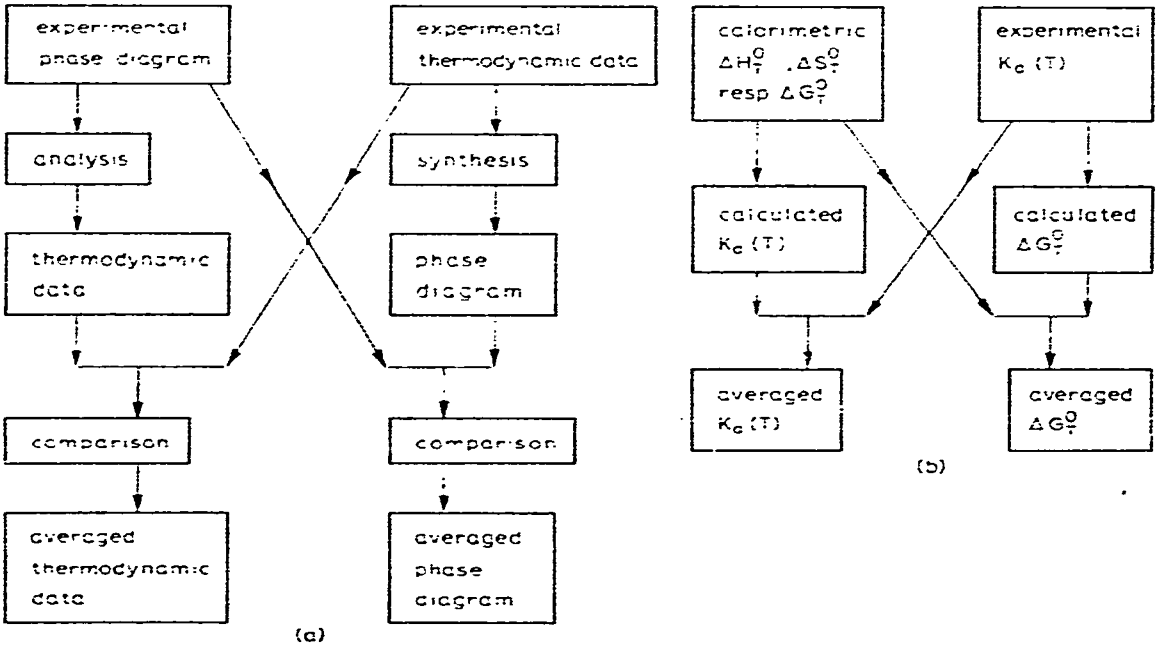

The methods of thermal analysis are applicable to direct observations of equilibria and also to the determination of thermodynamic quantities (enthalpy, specific heat, etc.). A direct study of phase equilibria is based upon the observation of the temperature (or pressure) at which the composition of a phase in a system undergoes a change. The study can be performed by direct observation (by microscopy) or by the methods of thermal analysis. The latter methods imply that the physical property which is measured represents all of the phase changes of the system. This property must be chosen so that the transformation is unambiguously reproduced, and should not be a summation of multiple phase changes which may take place in a parallel manner during the progress of a transformation.

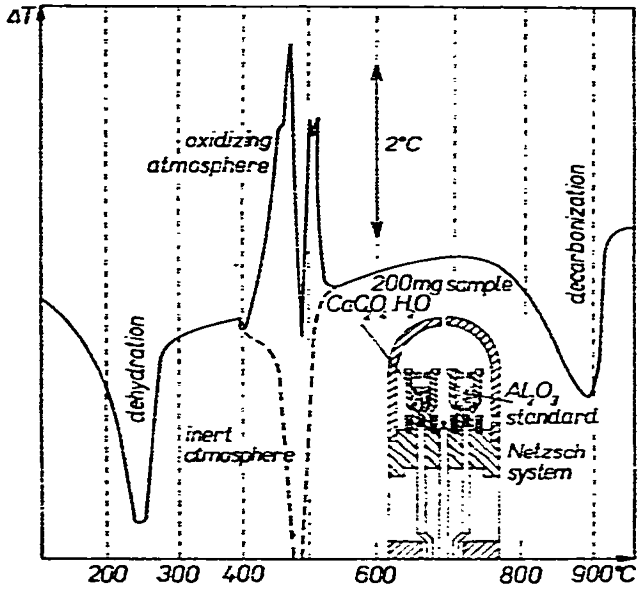

Fig. 2.1. Typical experimental DTA curve.

Figure 2.1 shows a typical case of the superposition of DTA curve peaks; curve 1 represents the decomposition of calcium oxalate and the oxidation of the released carbon monoxide. Only the decomposition is seen in inert atmospheres (dashed line).

The study of an equilibrium system utilizes two basic approaches, namely: (a) *static* methods and (b) *dynamic* methods. In static methods, equilibrium is established at a certain temperature as indicated by a constant value of the measured physical property in a sufficiently large time interval. In dynamic methods, the temperature is altered in a continuous way during the interval of a transformation and the instantaneous value of an appropriate parameter is recorded. The static method guarantees virtual equilibrium data, whereas dynamic methods involve various uncertainties. If the rate of transformation is slower than the rate of heating, the measured data do not correspond to the correct equilibrium states. Also, the phenomena of undercooling and superheating may lead to incorrect determination of the temperatures of equilibria. Hence, the kinetic phenomena should be carefully considered.

As a rule, the properties which are measured under dynamic conditions represent length, mass and enthalpy. It should be noted that the sensitivity of DTA methods is closely dependent on the heating rate. Some effects may disappear at very low heating rates as in the case of many ceramic materials while high heating rates for metallic materials have a similar consequence.

The methods of thermal analysis are applicable to the determination of thermodynamic data which are necessary for the evaluation of equilibria. The above-mentioned uncertainty, however, remains as a limiting factor. The small mass of sample and the extension of the temperature region for a single measurement has put the dynamic technique into a leading position in comparison with static methods. In order to measure the thermodynamic properties of materials, indirect methods are applied. These methods are based upon the investigation of rapid quenching (drop calorimetry). In the case of reversible transitions, the technique of freezing a high temperature composition is unsuitable. Dynamic calorimetry, however, makes it possible to observe any type of process.

2.2. Calorimetric measurements

2.2.1. Basic principles

The basic thermal properties of a material are described by the dependence of its

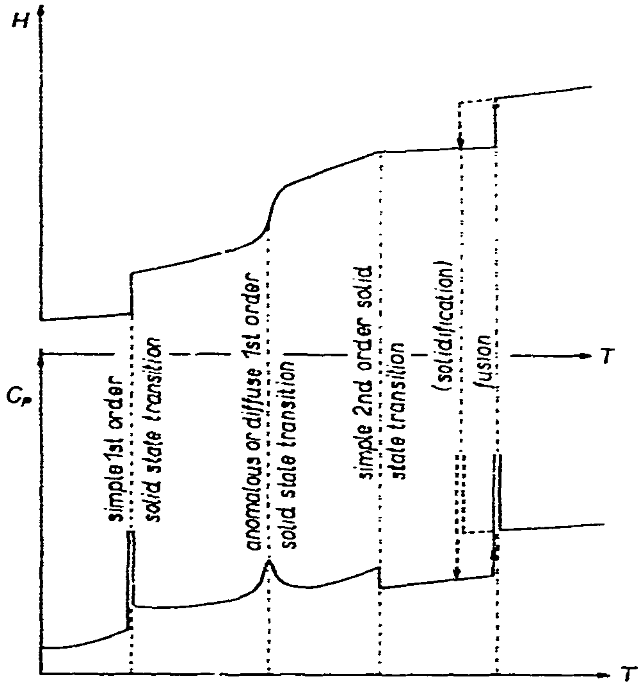

Fig. 2.2. Types of thermal behavior of matter; H, enthalpy; C_p, specific heat; T, temperature.

enthalpy upon temperature: the recorded curve facilitates the determination of characteristic temperatures and enthalpy changes of phase transitions (Fig. 2.2). Also, the specific heats of individual phases in the region of their presence may be determined as well.

A large number of different types of calorimeters have been described[1]. A simple calorimeter is made up of: a), a block; b), the sensing element; and c), the jacket. The block contains the measuring system and the source or the heat sink which makes it possible to generate or absorb heat in a well controlled manner. The sensing elements detect changes of temperature in the block, the jacket separates the block from the environment so that the enthalpic changes of the system become thermally isolated. In a twin calorimeter the difference of thermal behavior of the two systems is recorded, i.e., with two blocks placed in one jacket. The blocks may be located in a joint cavity or in separated holes of the jacket; the latter arrangement precludes heat exchange between the blocks. The process takes place in one of the two blocks while the other one with known thermal properties represents the reference. The jacket of the calorimeter may be kept at constant temperature which implies an "isoperibol" calorimeter. When the jacket is made time-dependent, the calorimeter becomes a nonstationary "scanning" type.

The measurement of enthalpy is realized in two ways: a) adiabatically, or b) diathermally. In an adiabatic system the block is thermally isolated from the jacket and the temperature changes of the block are measured during the reaction. In a diathermal system, heat exchange takes place between the block and the jacket and the heat flux is measured while the temperature of the system is an independent variable. This system is the basis of the scanning instrument and involves certain advantages such as a simple experimental arrangement and the small amount of sample. The measurement of heat flux is possible in two ways, as shown in Fig. 2.3. The jacket, which is the source of heat, is kept at temperature T_B, and the system which is being measured (with thermal capacity $C_{p,s}$) has the temperature T_s. The

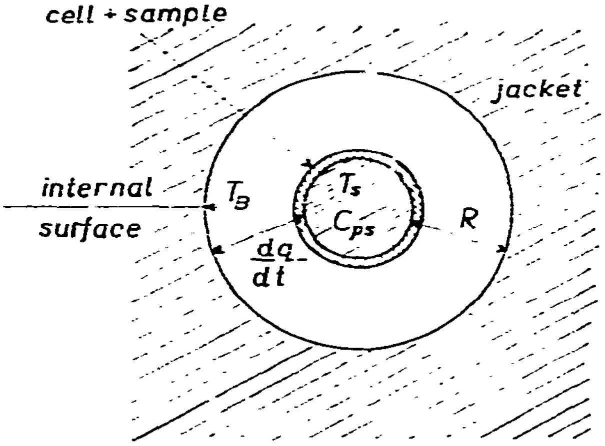

Fig. 2.3. Schematic diagram of a calorimeter.

heat flux, dq/dt, from the jacket to the system (block+sample) depends upon the thermal resistivity, R, along the path of heat transport. The heat flux may be determined either by recording temperature differences of the gradient on the thermal resistivity or by the measurement of the extra power which is emitted from an internal heater. This extra heater is applied to maintain a constant temperature gradient along the path of thermal resistivity.

The measurement of temperature differences is utilized in differential dynamic calorimetry (DDC), whereas differential scanning calorimetry (DSC) uses internal heaters. Both methods are an extension of DTA. It is now necessary to determine the limits of the basic DTA method by a theoretical analysis of the DTA curve.

2.2.2. *Theory of differential thermal analysis*

There are numerous books dealing with the theoretical background of DTA, such as Garn[2], Schultze[3], Wendlandt[5], and Berg[6], Pilojan[7], Smothers and Chiang[8], as well as review articles by Perron and Mathieu[4], Šesták and Berggren[9], Bohon[10], Gäumann and Oswald[11], Lugscheider[12], Heide[13], Berggren[14], etc. From the viewpoint of different approaches, they can be divided into two groups:

(a) Those assuming homogeneous distribution of temperature in both the sample and the reference, based on the work of Vold[15], Kerr and Kulp[16], Borchardt and Daniels[17], Kessis[18], Proks[19], Adam and Müller[20], and others.

(b) Those assuming the propagation of heat through both the sample and the reference, based on work of Boersma[21], Smyth[22], Soulé[23], Erikson[24], Lukaszewski[25], Berg and Egunov[26], Deeg[27] and others.

The second group is, in principle, the most reliable but unfortunately, the mathematical difficulties do not permit the inclusion of all of the experimental factors influencing the measurement. Simplifying assumptions must be made with the result that the theory can describe only the most simple case.

2.2.2.1. Homogeneous temperature distribution. The condition of homogeneous temperature distribution throughout both the sample and the reference can be achieved by studying liquids, as shown in Fig. 2.4. This system was first dealt with by Borchardt and Daniels[17] and later extended by Blumberg[28,29] for the heterogeneous reaction of silica glass with hydrofluoric acid. The sample and reference are placed in a thermostat of large thermal capacity, the temperature of which (T_3) rises linearly with time; stirring guarantees a homogeneous temperature distribution throughout the liquids (bath, sample and reference of temperatures T_3, T_1 and T_2, respectively).

In Borchardt and Daniels' theory[17] there are additional simplifying assumptions, such as:

a) Heat is transferred only by conduction.

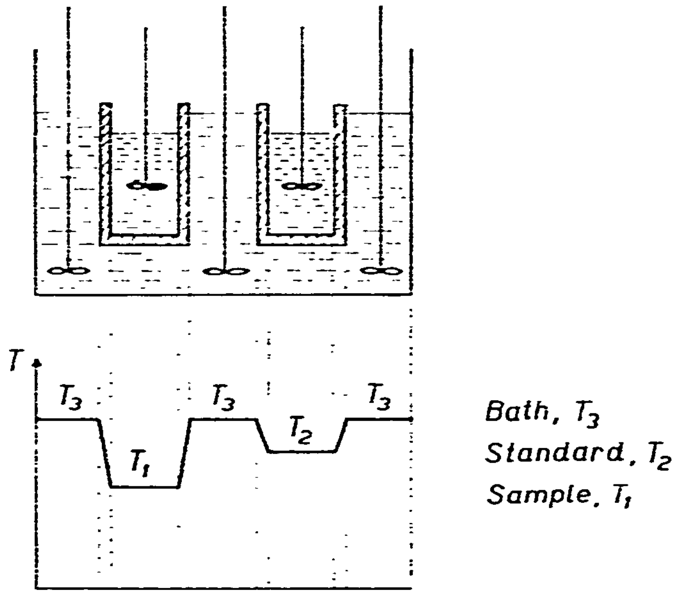

Fig. 2.4. Borchardt's apparatus; principle and temperature distribution curve.

b) Specific heat of the sample and the reference are equal as well as the coefficients of heat transfer (impedances *R–s* respectively) between the sample and the bath and between the reference and the bath.

c) Specific heats and coefficients of heat transfer are constant as well as the enthalpy change during the process investigated (temperature independent).

d) There is no heat exchange between the sample and the reference.

For an ideal case, a direct proportionality can be derived between the heat of reaction, ΔH, and the total area under the DTA peak, A, by $\Delta H = A/a$, where a is the thermal diffusivity (for $a = a_{\text{sample}} = a_{\text{reference}}$). A more general solution was given by Adam and Müller[20] and later by Kessis[18]. The advantage of this method is its capability to explain the shape of a DTA curve for invariant processes (phase transitions of 1st order) assuming a difference in the heat capacity and conductivity of the sample and reference (see Fig. 2.5). The thermostat is a metal block of large thermal

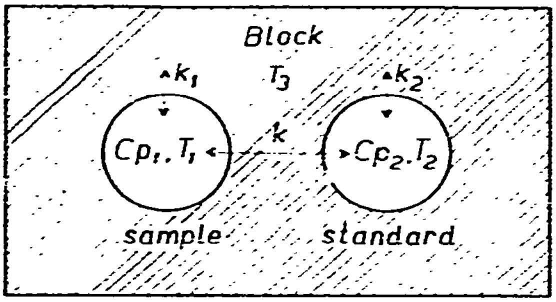

Fig. 2.5. A DTA block diagram with homogeneous temperature distribution in both specimens.

capacity with a homogeneous temperature distribution (T_3) which varies linearly with time. Two cells, containing the sample and the reference of thermal capacities C_{p_1} and C_{p_2}, and corresponding temperatures, T_1 and T_2, respectively, are located within the block. Defining the heat exchange between the block and the sample by the coefficient K_1, the block and the reference by K_2, and the reference and the sample by k, and assuming all coefficients are temperature independent, the equations for heat transport are:

$$C_{p_1}\frac{dT_1}{dt} = K_1(T_3-T_1)+k(T_2-T_1)+\psi \tag{2.1}$$

$$C_{p_2}\frac{dT_2}{dt} = K_2(T_3-T_2)+k(T_1-T_2) \tag{2.2}$$

where $\psi\ (= d\Delta H/dt)$ is the rate of heat generation or absorption in the reacting system. On introducing

$$\theta_1 = C_{p_1}/K_1, \quad \theta_2 = C_{p_2}/K_2, \quad \mathcal{K}_1 = k/K_1 \quad \text{and} \quad \mathcal{K}_2 = k/K_2 \tag{2.3}$$

Equations (2.1) and (2.2) can be rewritten as

$$\theta_1\frac{dT_1}{dt} + (1+\mathcal{K}_1)\,T_1 - \mathcal{K}_1 T_2 = T_3 + \frac{\psi}{K_1} \tag{2.4}$$

and

$$\theta_2\frac{dT_2}{dt} + (1+\mathcal{K}_2)\,T_2 - \mathcal{K}_2 T_1 = T_3\,. \tag{2.5}$$

As a first approach, it can be assumed that no heat exchange takes place between the sample and the reference ($k = 0$) and that the temperature rise of the block is linear with time, $T_3 = T_0 + \phi t$ (where ϕ is the constant heating rate). The initial temperature of the block, T_0, may be defined as equal to zero ($T_0 = 0$) so eqns. (2.4) and (2.5) change to

$$\theta_1\frac{dT_1}{dt} + T_1 = \phi t + \frac{\psi}{K_1} \tag{2.6}$$

and

$$\theta_2\frac{dT_2}{dt} + T_2 = \phi t\,. \tag{2.7}$$

If no heat effect is produced by the reacting system ($\psi = 0$), eqns. (2.6) and (2.7) can be integrated using initial conditions of $T = 0$ as $T_1 = T_{01}$ and $T_2 = T_{02}$, respectively, or

$$T_1 = \phi t - \phi\theta_1 + (\phi\theta_1 + T_{01})\exp(-t/\theta_1) \tag{2.8}$$

and

$$T_2 = \phi t - \phi\theta_2 + (\phi\theta_2 + T_{02})\exp(-t/\theta_2). \tag{2.9}$$

These equations demonstrate that after the crossing period where the exponential terms are a factor, the temperature of both cells rises linearly with time, lagging behind the temperature of the block by $\phi\theta_1$ for the sample, and by $\phi\theta_2$ for the reference. This temperature difference, $T_1-T_2=\Delta T$, which represents the baseline in the DTA curve, will be horizontal (parallel with the time axis) because of

$$\Delta T_B=\phi(\theta_2-\theta_1). \tag{2.10}$$

From the given model it becomes necessary to maintain a strictly constant heating rate, ϕ: in the case of parabolic heating (see section 4.1.2), ΔT_B becomes a linear function of temperature. If an exothermic or endothermic process takes place from the instant t_1, the ΔT curve returns back to the baseline by time t_2. Subtracting eqns. (2.6) and (2.7) gives

$$\theta_1\frac{d\Delta T}{dt}+\Delta T-(\theta_2-\theta_1)\frac{dT_2}{dt}=\frac{\psi}{K_1} \tag{2.11}$$

where $\Delta T=T_1-T_2$ and $d\Delta T/dt=(dT_1/dt)-(dT_2/dt)$. The temperature difference in DTA is usually measured with regard to the baseline, so that

$$\Delta T_R=\Delta T-\Delta T_B=\Delta T-\phi(\theta_2-\theta_1) \tag{2.12}$$

where subscripts R and B mean relative and basic, respectively. On combining eqns. (2.11) and (2.12)

$$\theta_1\frac{d\Delta T_R}{dt}+\Delta T_R+\left(\phi-\frac{dT_2}{dt}\right)(\theta_2-\theta_1)=\frac{\psi}{K_1} \tag{2.13}$$

At a constant heating rate, $dT_2/dt=\phi$, eqn. (2.13) reduces to

$$\theta_1\frac{d\Delta T_R}{dt}+\Delta T_R=\frac{\psi}{K_1} \tag{2.14}$$

Integrating eqn. (2.14) within the time interval limits (from t_1 to t_2)

$$\theta_1\,|\Delta T_R|_{t_1}^{t_2}+\int_{t_1}^{t_2}\Delta T_R\,dt=\frac{1}{K_1}\int_{t_1}^{t_2}\psi\,dt \tag{2.15}$$

the following proportionality is obtained

$$K_1A=\Delta H. \tag{2.16}$$

The first term of eqn. (2.15) is zero while the second represents the area of the DTA peak. Therefore, the peak area is proportional to the enthalpy change in the sample investigated.

For a particular analysis, a thermally invariant process can be chosen due to its relative simplicity. In the case where the sample temperature remains constant during the process (first-order transition described by the kinetic equation of zero reaction order), an equation can be written for the sample temperature,

$$T_1=T_{01}=-\phi\theta_1 \tag{2.17}$$

and for the reference

$$T_2 = -\phi\theta_2 + \phi t \tag{2.18}$$

hence $\Delta T_R = \phi t$. (2.19)

After the completion of the process, an exponentially shaped curve characterizes the return of the curve back to the baseline, as shown in Fig. 2.6. The height of the step h is directly proportional to the value of the heating rate ϕ, or

$$h = \phi\tau \tag{2.20}$$

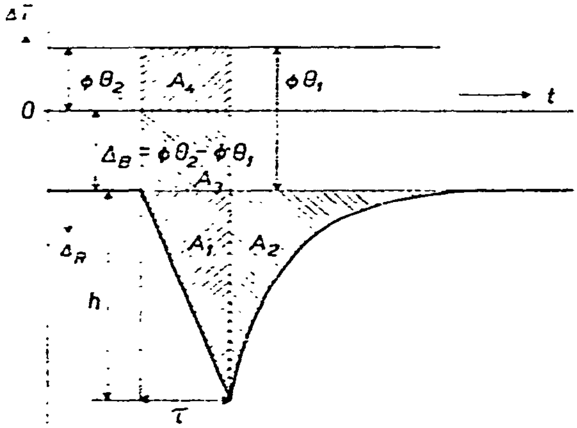

Fig. 2.6. Schematic representation of DTA peak for a first-order transition.

where τ is the duration of the process. The profile of the returning part of the DTA peak is given by the equation

$$\Delta T_R = \phi\tau\exp\left[\frac{-(t-\tau)}{\theta_1}\right] \tag{2.21}$$

The peak area can now be expressed in the above terms, or

$$A_1 + A_2 = A = \frac{\Delta H}{K_1} = \tfrac{1}{2}\phi\tau^2 + \phi\tau\theta_1 \tag{2.22}$$

where eqns. (2.20) and (2.21) are employed.

Many transformations are accompanied with a considerable change in the specific heat of the system, e.g. a change in θ_1. In the case of an invariant process, the sample temperature will generally be $T_1 = -\phi\theta_1 =$ constant ($T_3 = \phi t$). Although the constant, θ_1, corresponds to the sample material before the process, a different value of the constant, θ_1^*, will belong to the product after the process is complete. Hence, a different temperature difference, ΔT, will be created at the end of the process because of $\theta_1^* \neq \theta_1$ and a new baseline will be established (see Fig. 2.7). Thus

$$\Delta T_B^* = \phi(\theta_2 - \theta_1^*). \tag{2.23}$$

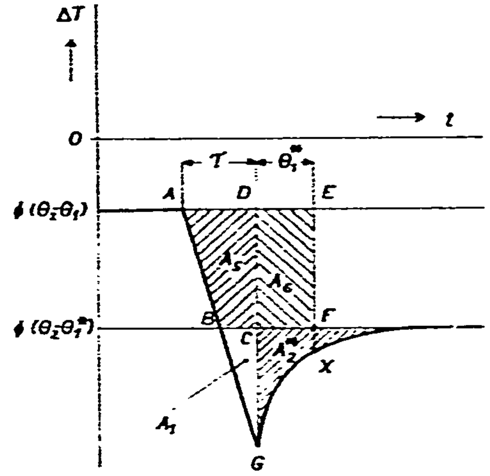

Fig. 2.7. Schematic representation of DTA peak for a first-order transition accompanied by a change of heat capacity of sample.

If θ_1 is a constant, then according to eqn. (2.22), $\Delta H/K_1 = A_1 + A_2$. Defining the new temperature difference, ΔT_R^* in the relation to the new baseline, ΔT_B^*, then

$$\Delta T_R^* = \Delta T - \Delta T_B^* \tag{2.24}$$

The point where the height of the signal, ΔT_R^*, decreases to the e^{-1}-th portion of its value at the peak maximum, can be designated as X. The distance, DE, in Fig. 2.7 then represents the value of θ_1^*. Assuming $\theta_1^* > \theta_1$, the area under the returning part of the peak can then be expressed as:

$$A_2^* = \overline{GC}\theta_1^* = \phi\tau\theta_1^* + \phi\theta_1^*(\theta_1 - \theta_1^*)$$

$$= \phi\tau\theta_1 + \phi\tau(\theta_1^* - \theta_1) + \phi\theta_1^*(\theta_1 - \theta_1^*) \tag{2.25a}$$

indicating

$$\phi\tau(\theta_1^* - \theta_1) = A_5 \text{ and } \phi\theta_1^*(\theta_1^* - \theta_1) = A_6 \tag{2.25b}$$

where

$$A_2^* = \phi\tau\theta_1 + A_5 - A_6 = A_2 + A_5 - A_6 \tag{2.25c}$$

which gives finally the relationship

$$\Delta H/K_1 = A_1 + A_2^* + A_6 - A_5. \tag{2.25}$$

This approach illustrates how to evaluate a DTA peak if the base line varies.

Kessis' theory[18] also considers the case where heat exchange occurs between the sample and the reference, which is very difficult to avoid in an ordinary DTA system. It is shown that if $K_1 = K_2 = \overline{K}$ and $\mathcal{K}_1 = \mathcal{K}_2 = \overline{\mathcal{K}}$, the DTA baseline remains horizontal, or

$$T_B = \phi \frac{\theta_2 - \theta_1}{1 + 2\overline{\mathcal{K}}} \tag{2.26}$$

where $\bar{\mathcal{K}}$ is the ratio between K and k (see eqn. (2.3)). Accordingly, the proportionality between the peak area and the system enthalpy remains unchanged, as given by

$$A = \frac{\Delta H}{\bar{K}(1+2\bar{\mathcal{K}})} \tag{2.27}$$

As can be anticipated, contact between the sample and the reference decreases the sensitivity and resolution of the DTA measurement. The proportionality between A and ΔH remains unchanged even if $\mathcal{K}_1 \neq \mathcal{K}_2$.

Similar conclusions were reached by Adam and Müller[20]. They derived a method for the direct determination of specific heats and their temperature dependence from a DTA curve. For a constant heating rate

$$\frac{dT_3}{dt} = \frac{dT_2}{dt} = \phi. \tag{2.28}$$

Assuming the equality of the heat transfer coefficients, $K_1 = K_2 = K$, it is valid that

$$\frac{C_p}{K} = \frac{\Delta T}{\phi} + \left[\frac{\Delta T}{\phi} + \frac{C_{p_2}}{K}\right] \frac{d\Delta T/dT_3}{1-(d\Delta T/dT_3)} \tag{2.29}$$

where C_{p_2} is the specific heat of the reference. If C_{p_2} and K are known, then the ΔT measurement is helpful in determining the value of C_p as a function of temperature, assuming that

$$\frac{d\Delta T}{\phi dt} = \frac{d\Delta T}{dT_3} \tag{2.30}$$

In the case, $d\Delta T/dt \ll \phi$, eqn. (2.29) simplifies to

$$\frac{C_p}{K} = \frac{\Delta T}{\phi}. \tag{2.31}$$

It should be emphasized that the above theories are applicable only for systems where the temperature distribution is homogeneous (i.e., in well-stirred liquid systems), or nearly homogeneous. For heterogeneous systems, the calculated results may deviate by as much as an order of magnitude, as was shown by Allison[30].

2.2.2.2. Temperature gradients in the sample body. In solid compacts a definite temperature gradient is created, as calculated by Smyth[22] (both specimens having identical thermal diffusivities, invariant process and infinite cylindrical geometry) and Tzusuki and Nagasawa[31].

For a first order reaction, as shown in Fig. 2.8, it can be seen that the temperature distribution before and after the reaction (similarly to that in the reference) does not change much (identical parabolas). During the reaction, on the other hand the heat supplied is consumed by the heat absorption due to the endothermal effect.

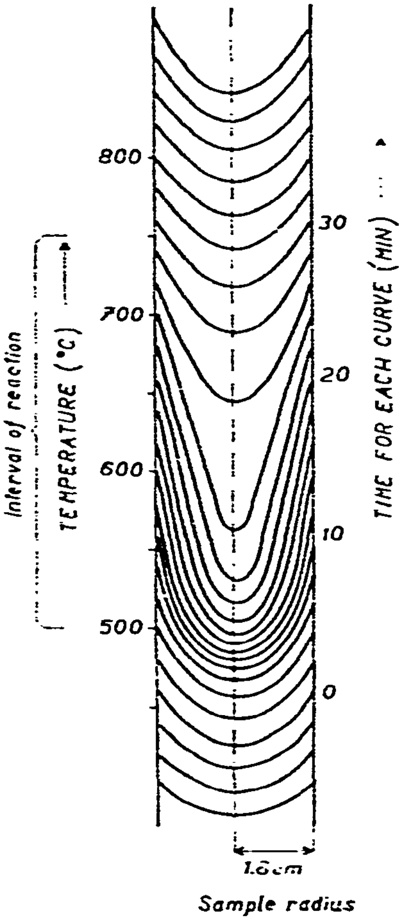

Fig. 2.8. Temperature distribution in a cylindrical solid sample during an endothermic process[31].

Assuming a temperature gradient in the reference, eqn. (2.1) can be changed to

$$\frac{1}{a_1}\frac{\partial T_1}{\partial t} = \nabla^2 T + \frac{1}{K_1}\frac{\mathrm{d}q}{\mathrm{d}t} \tag{2.32}$$

and also for the sample; eqn. (2.2) becomes

$$\frac{1}{a_2}\frac{\partial T_2}{\partial t} = \nabla^2 T \tag{2.33}$$

where ∇^2 is called Laplace operator and can be expressed for Cartesian coordinates, as

$$\frac{\partial^2}{\partial x^2} + \frac{\partial^2}{\partial y^2} + \frac{\partial^2}{\partial z^2}$$

and for cylindrical coordinates, as

$$\frac{\partial^2}{\partial r^2} + \frac{1}{r} \times \frac{\partial}{\partial r} + \frac{\partial^2}{\partial z^2}.$$

Assuming that the thermal diffusivity $a = a_1 = a_2$, then the function of the temperature difference, $T(= T_1 - T_2$, measured between the centers of the sample and the reference), can be obtained as

$$\frac{1}{a}\frac{\partial \Delta T}{\partial t} - \nabla^2 \Delta T = \frac{\psi}{K}. \tag{2.34}$$

Integration of eqn. (2.34) with respect to times gives (after Erickson[24] and later Boersma[21])

$$\frac{K}{a}(\Delta T_b - \Delta T_a) - K\int_{t_a}^{t_b} \nabla^2 \Delta T \mathrm{d}t = Q \tag{2.35}$$

where Q is the entire heat of the reaction per unit volume ($= \Delta H/V$). The first term on the left-hand side of eqn. (2.36) is evidently zero if the limits, subscripts a and b, are chosen before the beginning of the reaction and far after its completion, i.e., before and after the peak where $\Delta T_a = \Delta T_b = 0$. Integrating this equation over the volume V of the sample the peak area A is determined as

$$A = \int_{t_a}^{t_b} \Delta T \mathrm{d}t = BQ. \tag{2.36}$$

For a spherical cavity of the radius r_0 the value of $B = r_0^2/(6K)$, for a cylindrical cavity, $B = r_0^2/(4K)$, and for a slab of the height, h_0, $B = h_0^2/(2K)$. Erickson[24] has shown that for practical purposes in DTA, the temperature in the center of the sample is equivalent to that expected in an infinite cylinder (where $\mathrm{d}^2T/\mathrm{d}z^2 = 0$) if the length of the sample is at least twice its diameter. It behaves as a slab when the diameter of the disk-like sample is at least four times its length.

Melling et al.[32], investigated the influence of different physical parameters on the DTA peak shape by means of a computer. Their findings can be summarized here together with the previous mathematical results[21,24]. For a sample placed in the cavity of a conductive block:

(1) The area of the DTA peak is directly proportional to the heat of reaction and the mass of sample, but it is inversely proportional to the thermal conductivity of the sample material. It is dependent on the grain size and the packing of the sample.

(2) The DTA peak area, for ΔT vs. t, is independent of the applied heating rate.

(3) The reference peak temperature increases markedly with decreasing conductivity and increasing density and specific heat, if the reference physical properties remain constant for different sample properties. The sample peak temperature is, however, independent of conductivity but increases slightly with density and specific heat.

(4) Positioning of the thermocouples in the center of the sample (which has a small radius) does not affect the measured peak temperature but does influence the maximum differential temperature detected.

(5) With increasing sample radius, the peak area and the temperature difference is decreased resulting in distortion of the peak shape, as shown on a normalized case

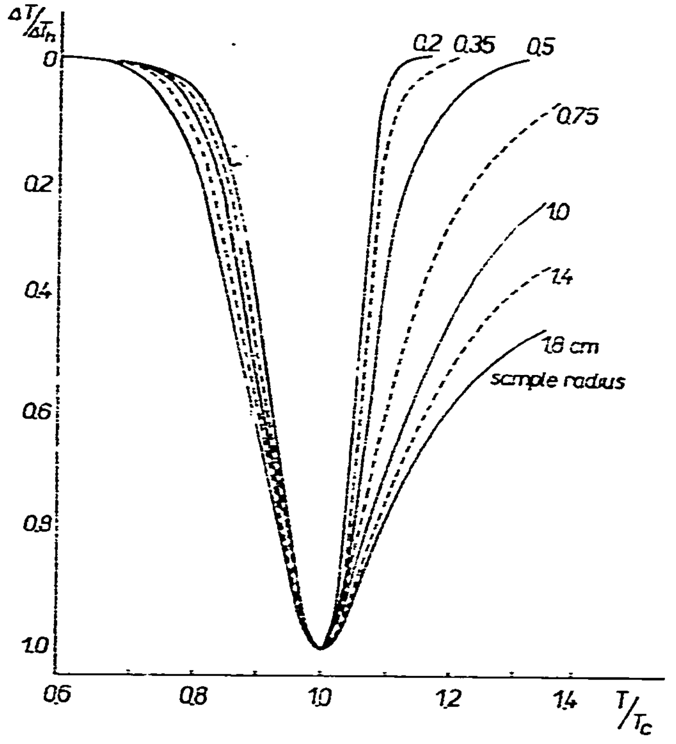

Fig. 2.9. Normalized DTA peak with regard to the temperature, T_c, and height, ΔT_h, occurring at the same point on the abscissa of the same magnitude to show the influence of varying sample radius[32].

in Fig. 2.9. Thus, samples of small radius are recommended for the determination of any reaction parameter.

For a different DTA experimental arrangement, schematically shown in Fig. 2.10, the problem of heat transfer was discussed by Lukaszewski[25]. All of the problems of DTA curves were discussed by Boersma[21], Smyth[22], Barrall and Rogers[33], Barshad[34], Jankovski[35], and de Jong[36].

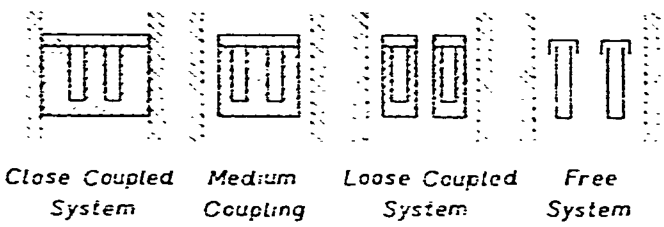

Fig. 2.10. Types of DTA sample and reference systems[25].

The influence of different physical properties of the reference and the sample on the general shape of the DTA curve, based on the work of Carslaw and Jaeger[37], shows that the temperature T_r at any radius r of an infinite cylinder of radius r_0, heated so that the periphery temperature increases at a constant heating rate ϕ, is given by

$$T_r = \phi\left[t - \frac{r_0^2 - r^2}{4a}\right]. \tag{2.37}$$

The temperature at the center, T_c, with regard to the temperature of the cylinder surface, T_s, is expressed as

$$T_c = T_0 + \phi\left[t - \frac{r_0^2}{4a}\left(1 - \exp\left(-\frac{4at}{r_0^2}\right)\right)\right] \tag{2.38}$$

where T_0 is the temperature at the beginning of heating. Hence, the temperature difference, ΔT, between the centers of the sample and the reference becomes

$$\Delta T = \frac{\phi r_0^2}{4}\left[\frac{1}{a_2} - \frac{1}{a_1}\right] - \frac{\phi r_0^2}{4}\left[\frac{1}{a_2}\exp\left(-\frac{4a_2 t}{r_0^2}\right) - \frac{1}{a_1}\exp\left(-\frac{4a_1 t}{r_0^2}\right)\right] \tag{2.39}$$

assuming no heat loss between the two materials. When t is larger, the second term on the right-hand side of eqn. (2.39) goes to zero, and

$$\Delta T = \frac{\phi r_0^2}{4}\left[\frac{1}{a_2} - \frac{1}{a_1}\right] \tag{2.40}$$

This equation was also derived by Pacor[38] to evaluate the sample diffusivity from the known ΔT deviation, the radius r_0, and the standard diffusivity a_2. He attempted to apply a modified eqn. (2.40) to the direct evaluation of ΔH. Unfortunately, this was applicable only for the DuPont system, where the conductivity K is larger than 10^{-3}, or

$$A \cong \frac{\phi r^2 \rho_1}{4K}\Delta H \cong \frac{\Delta H}{C_{p_1}}\left(\frac{\phi r_0^2}{4a_2} - \Delta T\right). \tag{2.41}$$

From the calibration of different DTA instruments with known compounds, Merzkanov et al.[39] recommended the equation,

$$\Delta H = C_p \frac{3.9\, C_{42} A}{r_0^2(1 + 2/\mathrm{Bi})} + 0.3\frac{W r_0^2}{C_{42}} \tag{2.42}$$

for $A = \int_0^{\infty} (\Delta T_c' - T_{c(t)})\,dt$, and $C_{42} = r_0^2/4(T_s - T_c)$,

and Biott number[39]

$$\mathrm{Bi} = \frac{\phi r_0^2}{[4C_{42}(T_0 - T_c) - \phi r_0^2]}$$

where T_0, T_c, T_n, T_s are the temperatures of the surroundings, the sample center, the sample holder (block) and the sample surface, respectively; $\Delta T_c'$ $(= T_c - T_n)$ is the temperature difference actually measured by thermocouples; $\Delta T_c(t)$ is the temperature difference scanned from the DTA peak; and W is the total thermal effect measured by the given apparatus per unit volume. Despite the rather extensive measuring techniques, these direct methods of evaluation have not provided sufficiently accurate data, particularly at temperatures above 400 °C. For temperatures above 600 °C the decrease of DTA sensitivity is evident, but this can be corrected by the equation

$$1/A = C_{43} + C'_{43}\bar{T}^3 + f(\bar{T}) \tag{2.43}$$

where C_{43}'s are constants and $\bar{T}$ is the mean temperature. Taking into account all of above phenomena, the best method of DTA peak evaluation is by means of calibration with known substances.

2.2.2.3. Calibration. In practice, the relationship between the DTA peak area and the change in the process enthalpy is influenced not only by the thermal properties of the sample and reference but also by their geometrical configurations, size, temperature detection and heating rate, and at least eighteen other effective parameters. In addition, the thermal properties of powder compacts are difficult to define well enough owing to the inhomogeneity and particle-size distribution which influence the material density. Therefore, no theory could include all these factors to correctly interpret the DTA curve. The only method to ensure good results is to calibrate the given apparatus with known substances even though such a calibration represents a rather difficult problem with respect to duplicating the precisely identical conditions for every experimental run. The proportionality factor in eqns. (2.16, 2.27, 2.36 and 2.37) and its temperature dependence can be determined for a given apparatus and experimental condition as follows:

(1) By comparison of the peak areas (A) with the reactions heats (ΔH) for a series of compounds in which the transitions take place within the temperature range desired[9,40,41]. Melting processes or solid–solid transitions are generally selected, as shown by Barshad[34]. Suitable compounds can be found in the work of Plato and Glasgow[42], Hedvall et al.[43], Wiedemann and van Tets[44], and others. A systematic error of calibration was dealt with by Sturm[189].

(2) Electrically by Joule heat generated in the sample as reported by Kleite and Viehman[45]; Dosch[45a] and Svoboda and Šesták[45b], the latter introducing a new system which permits a direct choice of the heat amount regardless the temperature dependence of the internal heater resistivity.

(3) Using the principle of the measurement of the rate of temperature equilibration after the reaction ceases. From a linear plot of the logarithm of instantaneous temperature difference vs. time, the apparent coefficient of heat transfer, K^*, can be determined from the slope of the line. The calibration constant is then found as a multiple of K^* with the specific heat of the sample, C_p (e.g. Bohon[10] and Berggren[14]).

(4) Application of an internal standard can also be used. MacAdie[46], Wiedemann[47] and Tarkar et al.[48], described the use of a standard either mixed with the sample or the reference. It is essential, of course, that such a standard should not disturb the entire process investigated.

(5) Berg's method[26,40] of calibration in which the heats of phase transitions

TABLE 2.2

STANDARD SUBSTANCES USED FOR DTA CALIBRATION

Compound	*Equilibrium temperature from tables*	*ICTA*[49] *onset temperature DTA expts.*	*ICTA*[49] *peak temperature DTA expts.*	*Ratio of* ΔH *compound vs.* ΔH K_2SO_4[a] *from tables*	*Ratio of exp.* ΔH *comp. by DTA*[b] *vs.* ΔH K_2SO_4 *from tables*
KNO_3	127.7	128±5	135±6	—	—
In	157	154±6	159±6	—	—
Sn	231.9	230±5	237±6	—	—
$KClO_4$	299.5	290±6	309±8	1.69	1.7 ±0.01
Ag_2SO_4	430	424±7	433±7	0.97	2.25±0.02
SiO_2	573	571±5	574±5	0.08	0.09±0.01
K_2SO_4	583	582±7	580±6	1.0	1.04±0.14
K_2CrO_4	665	665±7	673±6	1.26	1.0 ±0.06
$BaCO_3$	810	808±8	819±8	2.33	2.28±0.07
$SrCO_3$	925	928±7	938±9	2.42	2.27±0.15

[a] ΔH K_2SO_4 = 1.94 kcal/mol, as taken from *Circ. US Nat. Bur. Stand.*, No. 500 (1952). [b] Compiled from the average data reported in ref. 50 and by M. Nevřiva and P. Holba, *Proc. 6th Czech. Conf. Thermal. Anal. 1973*, SVŠT, Bratislava, 1973, p. S79–S85.

from multiple DTA curves may be calculated based on two runs; one with the original material and the second with the material diluted with an inert substance.

During these calibrations, the requirements of the Committee on Standardization of ICTA[49] should be taken into account and the recommended standards in Table 2.2 should be used[49,50]. In addition, a 4:1 by weight mixture of SiO_2 and K_2SO_4 is recommended to evaluate the ability of a given apparatus to resolve two thermal effects occuring about 10°C apart. Maximum sample size should not exceed 300 mg. The Al_2O_3 should be calcined at 1200°C and stored over P_2O_5. The heating

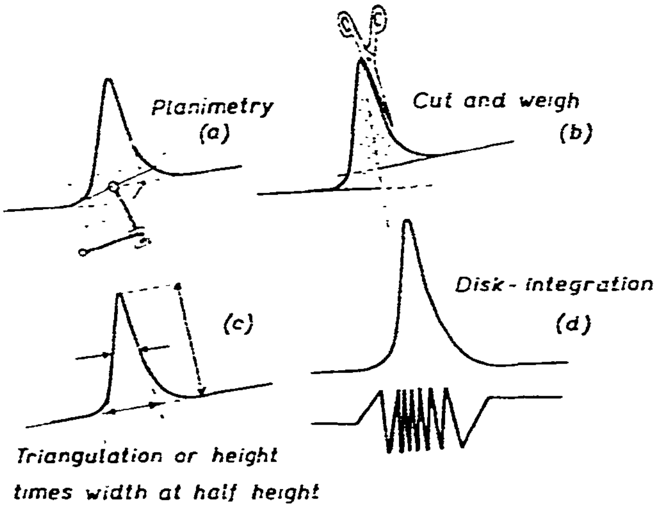

Fig. 2.11. Schematic representation of DTA peak area integration.

rates between 3–10°C/min are most convenient with the operating conditions of each instrument employed in accordance with the instrument's instruction manual. The different methods of peak area evaluation are schematically shown in Fig. 2.11. Method (c) is of a use only in some "ideal" cases such as micro-DTA.

2.2.3. *Theory of differential dynamic calorimetry*

The differential dynamic calorimetry (DDC) technique was developed from DTA by replacement of the temperature sensing thermocouple junction from inside of the specimen to its outer surface. Thus, only the changes in the system enthalpy are detected in contrast with "classical" DTA where the changes in the sample thermal conductivity are also determined. Therefore, the DDC arrangement has removed the errors introduced by particle-size effects, coalescence of particles, etc., as discussed by Boersma[21]. The DDC technique, as first introduced by Schwiete and Ziegler[51] and later Faktor and Hanks[52], has proved to be useful for the measurement of enthalpic changes as low as 1 cal with a reported accuracy of ±4 percent. The sample and the reference are placed separately into two cells (sample-holders), usually provided with covers to limit unwanted convection currents (see Fig. 2.10 (d)). The temperature is sensed on the cell-wall by a thermocouple junction in contact with the sample holder wall. The sensitivity of this arrangement, unfortunately, is less than that of DTA, particularly at higher temperatures.

The theoretical description of DDC is based on the work of Faktor and Hanks[52]. Neglecting the heat exchange between the sample and the reference, the following equation for enthalpy change can be written for each cell

$$\mathrm{d}H/\mathrm{d}t = \xi_f - \xi_b \tag{2.44}$$

where ξ_f is the heat flux along the direction from the furnace internal surface and ξ_b is the heat flux lost by the thermocouple wires and their supports. The enthalpy increase for a system where no reaction occurs is proportional to the temperature change

$$\mathrm{d}H = C_\mathrm{p}\mathrm{d}T \tag{2.45}$$

where C_p is the average thermal capacity of the sample and its holder. Heat supply from the surrounding heater is carried out mainly by conduction and radiation and can be expressed by

$$C_\mathrm{p}\frac{\mathrm{d}T}{\mathrm{d}t} = K_1(T_\mathrm{f}-T)+K_2(T_\mathrm{f}^4-T^4)-K_3(T-T_\mathrm{b}) \tag{2.46}$$

and

$$C_\mathrm{p}\frac{\mathrm{d}(T+\Delta T)}{\mathrm{d}t}+\psi = K_1(T_\mathrm{f}-T-\Delta T)+K_2(T_\mathrm{f}^4-(T+\Delta T)^4)-K_3(T+\Delta T-T_\mathrm{b}) \tag{2.47}$$

for the reference and sample, respectively, assuming the same values of C_p, K_1, K_2

and K_3 for both cells. The symbols employed are: T_f = temperature of the furnace internal surface surrounding the specimens; T_b = temperature of cell bottom wall where temperature is detected; K_1 and K_2 = transmission coefficients for conduction and radiation, respectively; and K_3 = transmission coefficient for heat transport along thermocouples, and $\psi = \mathrm{d}\Delta H/\mathrm{d}t$ = production of heat. Combining eqns. (2.46) and (2.47), and neglecting higher T powers

$$C_p \frac{\mathrm{d}\Delta T}{\mathrm{d}t} + \psi = -(K_1+K_3+4K_2T^3)\,\Delta T. \tag{2.48}$$

Assuming the same baseline before and after the peak and $\Delta T = 0$, integration of eqn. (2.44) yields

$$\Delta H = -\left[(K_1+K_3)+4K_2T^3\right]\int_0^t \Delta T \mathrm{d}t = (P+QT^3)\int_0^t \Delta T \mathrm{d}t. \tag{2.49}$$

For an invariant process (e.g., fusion or solidification of Cd metal[152]) taking place in a narrow temperature interval, the expression $(P+QT^3)$ can be assumed as temperature independent which introduces an error of about 5 percent. The sensitivity of the measurement, $\tilde{S}$, defined as the peak area per one calorie, is given by

$$\tilde{S} = \frac{\int_0^t \Delta T \mathrm{d}t}{\Delta H} = \frac{A}{\Delta H} = \frac{1}{(K_1+K_3+4K_2T_m^3)} \tag{2.50}$$

and is dependent on the mean temperature of the DDC peak, T_m.

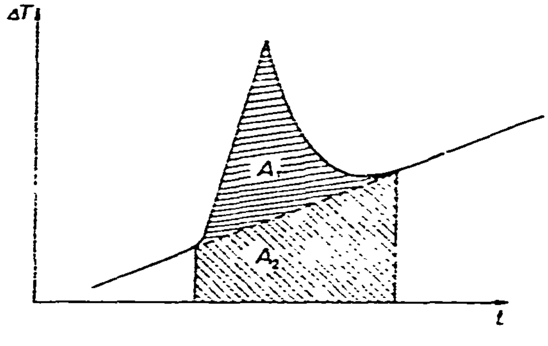

Fig. 2.12. Typical DDC curve.

If the quantities, C_p, K_1, K_2 and K_3, change during a first-order process by $\delta C_p'$, $\delta K_1'$, $\delta K_2'$ and $\delta K_3'$ for the reference, and δC_p, δK_1, δK_2 and δK_3 for the sample, then eqn. (2.48) changes to

$$\frac{\mathrm{d}\Delta H}{\mathrm{d}t} = \psi = -\left[(K_1+K_3+\delta K_1'+\delta K_3')+(4K_2+4\delta K_2')T^3\right]\Delta T - \tag{2.51}$$

$$-(\delta K_1-\delta K_1')(T_f-\mathrm{T})-(\delta K_2-\delta K_2')(T_f^4-T^4)-$$

$$-(\delta K_3-\delta K_3')(T-T_b)-(\delta C_p'-\delta C_p)\frac{dT}{dt}-(C_p-\delta C_p')\frac{d\Delta T}{dt}. \quad (2.52)$$

After integration

$$\begin{aligned}\Delta H = &-[(K_1+\delta K_1')+(K_3+\delta K_3')+(K_2+\delta K_2')\,4T^3](A_1+A_2)-\\&-\int[(\delta K_1-\delta K_2')(T_f-T)+(\delta K_2-\delta K_2')(T_f^4-T^4)-\\&-(\delta K_3-\delta K_3')(T-T_b)]\,dt-\int(\delta C_p'-\delta C_p)\,dT-\int(C_p+\delta C_p')\,d\Delta T \quad (2.53)\end{aligned}$$

where A_1 and A_2 are the areas to be determined, according to Fig. 2.12. In the case of no thermal effects, $A_1=0$ and A_2 is equal to the sum of the last three integrals on the right-hand side of eqn. (2.53). Accordingly (see Fig. 2.12),

$$\Delta H = -[K_1+\delta K_1'+K_3+\delta K_3'+(K_2+\delta K_2')\,4T^3]\,A_1 \quad (2.54)$$

It should be mentioned that most of the DTA systems commercially produced are designed as DDC systems.

2.2.4. *Theory of differential scanning calorimetry*

The method of DSC, as previously discussed in Section 2.2.1, is based on compensation measurements of heat fluxes. This system was first introduced by Eyraud[53,54] for a twin calorimeter, where the specimens were heated in such a way so as to ensure minimum temperature difference between the sample and the reference under a constant rate of temperature increase. If an endothermic process takes place the maintenance of a zero temperature difference requires introduction of an increment of heat into the sample at a rate which balances the internal temperature consumption. This extra heating is then recorded as a function of time or temperature, respectively. Eyraud obtained the internal heating by passing an electric current through the sample which was mixed with graphite powder while Speros and Woodhouse[55] used a platinum wire heater inserted into the sample. A sensitivity of enthalpy measurement as low as ±0.4 rel. percent has been reported with the DuPont and Perkin–Elmer instruments[56]. These instruments have been described by Baxter[57] (DuPont) and O'Neill and Gray[58,60,62] (Perkin–Elmer).

The most instructive DSC theory seems to be that of Gray[59] and David[61] based on the conservation of energy and the linear dependence of heat flow to temperature gradients, which may explain classical DTA as well. Assuming the sample to have a uniform temperature, T_1, total heat capacity (sample cell), C_{p_1}, and surrounding temperature (the bath as a heat source), T_B, then the thermal energy flow, dq/dt, to or from the sample is controlled by a certain thermal resistance, R. The temperature difference between the sample and its surroundings gives rise to an equation referred to as Newton's law (compare Fig. 2.3)

$$\frac{dq}{dt}=\frac{T_B-T_1}{R} \quad (2.55)$$

This is the thermal analogy of Ohm's Law for a potential difference across an electrical resistance. During a thermal process, the heat generated by the sample is positive and heat absorbed is negative, the rate of the latter is dh/dt. The energy generated in the sample can either increase the sample temperature or be lost to the surroundings so the heat balance yields

$$\frac{\mathrm{d}h}{\mathrm{d}t} = C_{\mathrm{p}_1}\frac{\mathrm{d}T_1}{\mathrm{d}t} - \frac{\mathrm{d}q}{\mathrm{d}t} = C_{\mathrm{p}_1}\frac{\mathrm{d}T_1}{\mathrm{d}t} - \frac{T_1 - T_{\mathrm{B}}}{R} \tag{2.56}$$

The maintenance of the condition of specimen temperature equality in energy per unit time which the sample absorbs from or provides to the sample-holder heater must be compensated for by a corresponding variation in the differential electrical power, being equivalent to the measured dq/dt. Using eqn. (2.56) together with the time derivative of eqn. (2.55), a basic DSC equation can be obtained[59] relating the change in the sample enthalpy, dh/dt, to the DSC variable, dq/dt

$$\frac{\mathrm{d}h}{\mathrm{d}t} = -\frac{\mathrm{d}q}{\mathrm{d}t} + (C_{\mathrm{p}_1} - C_{\mathrm{p}_2})\frac{\mathrm{d}T_{\mathrm{B}}}{\mathrm{d}t} - RC_{\mathrm{p}_1}\frac{\mathrm{d}^2 q}{\mathrm{d}t^2} \tag{2.57}$$

The term, dh/dt, involves the sum of three terms: the first being the signal measured from the zero baseline; the second the baseline displacement due to heat capacity mismatch between the sample and the reference; and the third term is the slope of peak normal multiplied by a constant RC_{p_1}. It can be seen that the area under the DSC peak is equal to the change in reaction enthalpy, $\Delta q = -\Delta h$, and that the value of an instrument empirical constant, R, is not required. The calibration is therefore not dependent on the temperature and a single point of calibration applies over the whole range. By decreasing the value of R, the accuracy and sensitivity of the DSC apparatus is increased[61]. A thermally invariant process illustrates the DSC curve of the type shown in Fig. 2.13. For the linear part, where the transition rate is time independent, the following equation is valid

$$\frac{\mathrm{d}q}{\mathrm{d}t} = (C_{\mathrm{p}_1} - C_{\mathrm{p}_2})\frac{\mathrm{d}T_{\mathrm{B}}}{\mathrm{d}t} + \frac{1}{R}\frac{\mathrm{d}T_{\mathrm{B}}}{\mathrm{d}t}t\,. \tag{2.58}$$

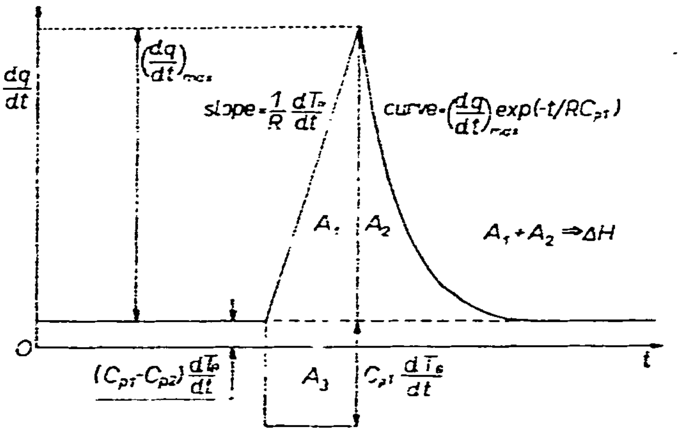

Fig. 2.13. Schematic representation of DSC peak for a first-order transition[59].

The straight-line slope is then equal to the scanning rate divided by the thermal resistivity. The peak height will rise with the decreasing value of R, or

$$\left(\frac{\mathrm{d}q}{\mathrm{d}t}\right)_{\max} = \frac{1}{R}\frac{\mathrm{d}T_B}{\mathrm{d}t}\,t_{\max} = \frac{\phi}{R}\,t_{\max}. \tag{2.59}$$

The advantage of the DSC system may be best shown by comparing it with DTA using the same approach[59]. Writing an equation equivalent to eqn. (2.56) but for the standard cell (subscript 2) where $\mathrm{d}h/\mathrm{d}t = 0$, mutual substraction and rearrangement gives

$$R\frac{\mathrm{d}h}{\mathrm{d}t} = (T_1 - T_2) + R(C_{p_1} - C_{p_2})\frac{\mathrm{d}T_2}{\mathrm{d}t} + RC_{p_1}\frac{\mathrm{d}(T_1 - T_2)}{\mathrm{d}t}$$

$$= \Delta T + R(C_{p_1} - C_{p_2})\,\phi + RC_{p_1}\frac{\mathrm{d}\Delta T}{\mathrm{d}t}. \tag{2.60}$$

This assumes the same R for both specimens as well as a constant scanning rate, $\mathrm{d}T_2/\mathrm{d}t = \mathrm{d}T_B/\mathrm{d}t = \phi$.

The term, $R\,\mathrm{d}h/\mathrm{d}t$, is again the sum of three terms: the first is the temperature difference recorded; the second represents the baseline displacement from the zero signal level; and the third term is the slope of the curve at any point multiplied by a constant, RC_{p_1}. This constant has the units of time and is in fact the thermal time

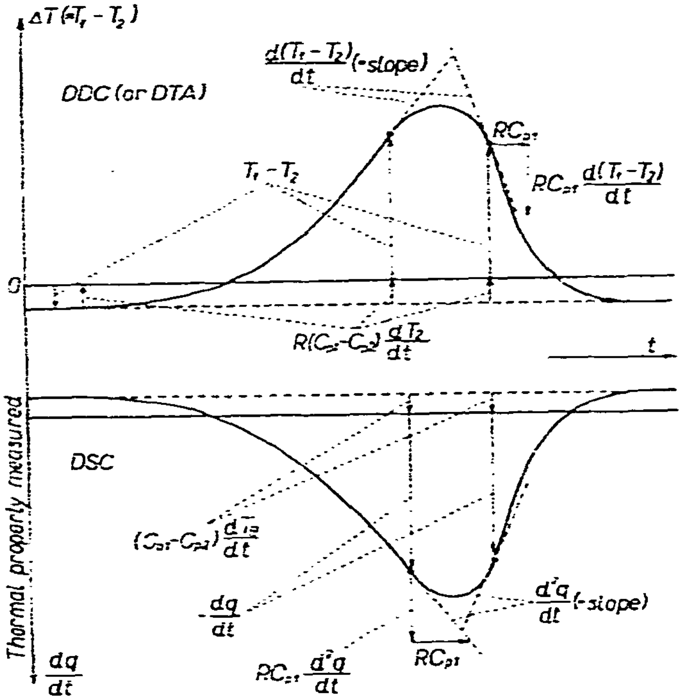

Fig. 2.14. Comparison of DTA and DSC measurements and their significance (according to Gray[59]).

constant of the system; it is very important. It should be noted that the recorded signal, ΔT, is proportional to R for a given sample size while that of a DTA apparatus is designed to have R equal to zero at no signal. The requirements of high inherent sensitivity, which requires a large R, is therefore incompatible with the demand for fast response or high resolution which needs RC_{p_1} as small as possible. It can be seen that the area under the DTA peak is only proportional to the change in reaction enthalpy, $R\mathrm{d}h = \Delta T \mathrm{d}t$, and thus the value of R and its temperature variation should be established.

The quantity, $\mathrm{d}h/\mathrm{d}t$, is composed of three terms in both the DSC and DTA techniques and their meanings are illustrated in Fig. 2.14. The fundamental reason for the differences in DTA and DSC curves is that the DTA system is a temperature measuring device and energy information is reached through secondary relationships from the sample temperature variation. The DSC apparatus is an energy measuring device where the sample temperature is monitored and maintained equal to the program heating. It should be noted that the empirical constant, R, occurs only in the third term of the right-hand side of eqn. (2.57) in contrast to eqn. (2.60). It is possible to decrease the thermal time constant by reducing R without sacrificing sensitivity, which is the principal design objective for a differential scanning calorimeter, as demonstrated in Fig. 2.14 (for a sharp time independent transition, compare Fig. 2.13). In DSC experiments, the peak area is not changed on decreasing R while in DTA, the peak area is reduced. The calibration of a DSC apparatus is usually accomplished by metals[61] and the average reported accuracy is about ±1 rel. percent.

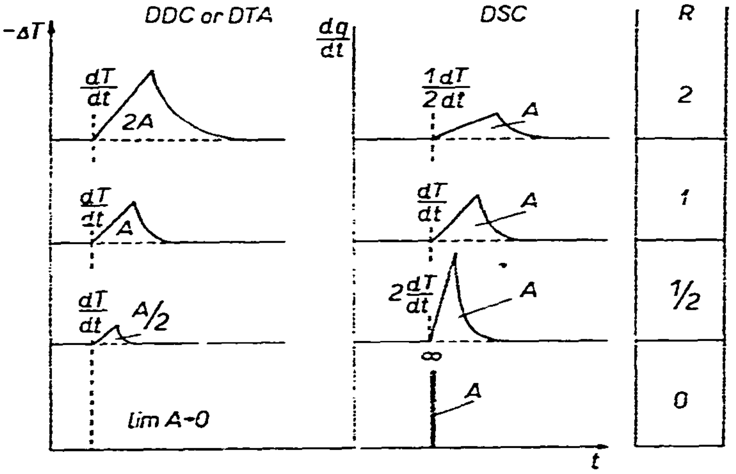

Fig. 2.15. Comparison of sensitivity of DTA and DSC methods (according to Gray[59]).

The determination of the specific heat of a sample is based on the second term on the right hand side of eqn. (2.57), as illustrated in Fig. 2.16. The rate of heat flow to the sample, of specific heat, C_{p_1}, and mass, m_1, is given by

$$\frac{\mathrm{d}q}{\mathrm{d}t} = m_1 C_{p_1} \frac{\mathrm{d}T}{\mathrm{d}t}. \qquad (2.61)$$

After the apparatus is calibrated, the distance, y, is directly proportional to $\mathrm{d}q/\mathrm{d}t$ in cal/sec. Another method is to calibrate the apparatus by a known material of given function, $C_p = \mathrm{f}(T)$, instead of a sample. For an arbitrary temperature, then

$$K\,y = m\,C_p \frac{\mathrm{d}T}{\mathrm{d}t} \text{ and/or } Ky' = m'\,C'_p \frac{\mathrm{d}T}{\mathrm{d}t} \tag{2.62}$$

where K is the calibration constant, see Fig. (2.16). On dividing the equations, we obtain

$$\frac{C_p}{C'_p} = \frac{m'\,y}{m\,y'}. \tag{2.63}$$

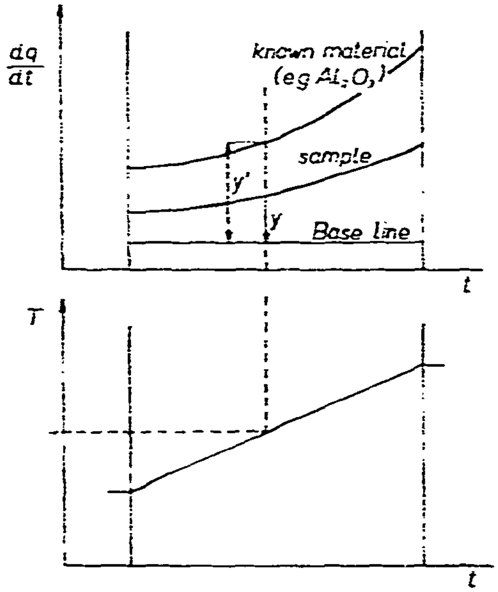

Fig. 2.16. Principle of specific heat determination.

Using the entire DSC curve, the temperature dependence of C_p in a given temperature interval may be established by the equation, $C_p = a + bT + cT^{-2}$. According to O'Neil[58], the accuracy of C_p determination is about ± 0.3 rel. percent or better, which is close to that obtained by adiabatic calorimetry; however, the sample size and the working time are much less. The accuracy is dependent upon the temperature gradient between the sample and its holder. For samples of high thermal conductivity it can be as good as ± 0.1 rel. percent, while for samples of a poor conductivity (polymers), it may decrease to about ± 5 rel. percent.

Commercially produced DSC instruments enable measurements to be made to a temperature of 600°C; for high temperature calorimetry, the instruments described by Speros and Woodhouse[55] (600–800°C) and Nicholson and Fulrath[64] (900–960°C) may be used. Other examples of DSC utilization are given in references[65–68].

2.3. *Measurements of other thermophysical properties*

In addition to calorimetrically determined properties, other important quantities such as thermal expansion, compressibility, and vapor pressures are of considerable interest from the point of view of chemical thermodynamics. Most of these properties are preferably determined by means of dynamic techniques.

2.3.1. *Thermal expansion*

The coefficient of the volume thermal expansion is defined as[69]

$$\alpha_V = \frac{1}{V_0}\left(\frac{\partial V}{\partial T}\right)_P \qquad [K^{-1}] \tag{2.64}$$

and the coefficient of linear expansion

$$\alpha_L = \frac{1}{L_0}\left(\frac{\partial L}{\partial T}\right)_P \qquad [K^{-1}] \tag{2.65}$$

where V is the volume and L is the length. Both coefficients are usually approached as linear functions of temperature but the average values are calculated in a given temperature interval, or

$$\bar{\alpha}_L = \frac{1}{L_0}\frac{\Delta L}{\Delta T}. \tag{2.66}$$

It can be shown that $\bar{\alpha}_V = 3\bar{\alpha}_L$. For single crystals, α_L depends on the crystallographic direction; only cubic structures have a constant coefficient of thermal expansion in any direction. For anisotropic materials, it is necessary to consider the expansions along all three crystallographic axes.

For the measurement of thermal expansion, five different methods may be employed[69,70]. The first three are based on the measurement of length changes of a rod by a detecting system such as a dial gauge[71-73], combination of a telescope system with micrometer[74], interferometer[75], and mirror reflection[74]. Other methods are based on the lattice constant measurement by X-ray diffraction[76] and/or volume measurements of a known system containing the sample[77], or directly from sample density[78,79]. Dynamic techniques are more common[80], the theory of which is given by Reiss[81]. Some dilatometric measurements of organic glasses have also been made[82-84].

The relationship between α and the other thermodynamic quantities was determined by Grüneisen[85] and later simplified by Eastabrook[86], as

$$\alpha_V = -\frac{C_v}{T\mathcal{K}_T}\left(\frac{\partial T}{\partial V}\right)_S = \frac{C_v}{V\mathcal{K}_T}\gamma \tag{2.67}$$

and

$$\gamma = -\frac{V}{T}\left(\frac{\partial T}{\partial V}\right)_S = -\left(\frac{\partial \ln T}{\partial \ln V}\right)_S \tag{2.68}$$

where γ is Grüneisen's constant to be calculated on the basis of Debye's model of a solid. Within the temperature interval, $T = 0.2\,\theta_D$, $T = \theta_D$, the constant $\mathcal{K}_T$ may be assumed to be temperature independent provided that θ_D is the Debye temperature; C_v is the heat capacity at the constant volume, V.

2.3.2. Determination of the integral heat of sorption

Schreiber[87] has used the measurement of the heat of sorption for the determination of specific surface area of powders. For this measurement, the principle of DTA was found suitable[190]. The constant ratio of the specific surface area and the integral heat of sorption for a given system (adsorbate, adsorbent and temperature) is determined experimentally by means of calibration with a suitable material of known specific surface area.

2.4. Direct investigation of equilibria

For the study of equilibrium states it is possible to employ any property of the system if this property indicates unambiguously the change of phase composition. The enumeration of individual methods is not the aim of this section and hence only the most useful techniques and the typical methods of interpretation are included. The methods are classified according to the processes investigated. The same course of utilization of the individual techniques is faced in practice[70].

2.4.1. Study of condensed systems

High-temperature Microscopy is based on the direct observation of the creation and/or disappearance of a particular phase in a system under dynamic temperature conditions[88]. The best example is the classical method of the melting point determination of organic substances[89] placed in a glass capillary tube inside a temperature controlled bath or block. An automatic apparatus was described by Muller and Zenchelski[90] and later by Furst and Shapiro[91]. A survey of methods for the determination of melting point and their comparison with other conventional techniques have been given[92–99]. For specific purposes a polarizing microscope is necessary such as in the study of the transformations of NH_4NO_3 (ref. 96), cholesteryl esters of higher organic acids[94], or chemical reactions such as the dehydration of calcium sulphate dihydrate to the hemihydrate in presence of liquid water[100]. The change in intensity of transmitted light or light shaded by the sample body (optical dilatometry) may also be detected instrumentally[101–103].

Dilatometry has a wide use in the investigation of solid–solid transformations which[104–109] arise from a discontinuity in the dilatometric curve, such as the $\alpha \rightarrow \beta$ transition in SiO_2 (ref. 106), NH_4NO_3 (ref. 107), transitions in metallic whiskers[105], and ZrO_2 (ref. 109), as illustrated in Fig. 2.17a.

Phase transitions of the second order show up a break in the dilatometric curve, as shown in Fig. 2.17c. Other examples are in ferroelectric $NaNO_2$ (ref. 108), trans-polybutylene[110], ferrites[111], and the determination of glass-transition temperature such as glassy selenium[114] and organic[113] and inorganic glasses,[115,116] (Fig. 2.17b). The study of chemical processes such as gypsum dehydration in an autoclave in the

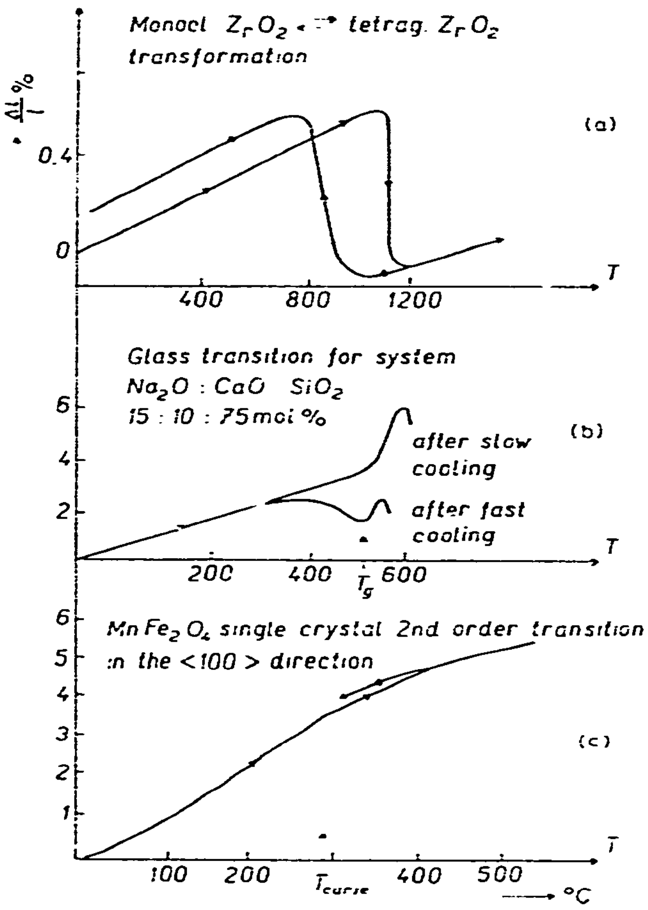

Fig. 2.17. Typical dilatometric curves. a, modified first order transformation; b, glass transition; c, second order transition[110].

presence of liquid water[112,117] can also be determined. The use of volume dilatometers has been given[77,118].

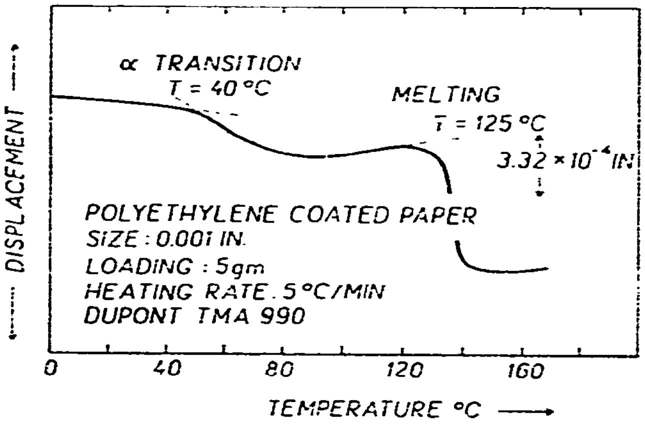

Fig. 2.18. Thermomechanical analysis curve taken from ref. 122.

Emanation Thermal Analysis is based on the measurement of the rate of release of inert radioactive gases previously incorporated into the solid[119–121]; it is a very sensitive method for the detection of transformation temperatures, such as the Fe_2O_3 calcination[119] and solid state reactions in the systems[120,121] $BaCO_3+TiO_2$, $CaO+Fe_2O_3$, KCl–$CaCl_2$ and $CaSO_4$–$BaSO_4$.

Thermomechanical Analysis provides a useful measurement of the mechanical changes which occur within a material as a function of temperature by the probe tip penetration of the sample, etc. Besides the determination of phase transition and softening temperatures, a number of other important phenomena such as compression and tensile modulus or expansion coefficients may also be determined[122]. A typical curve is shown in Fig. 2.18.

High Temperature X-ray Diffractometry is a selective method for determining phase transitions, regions of phase thermal stability, reaction reversibility, etc. The dynamic mode utilizes the measurement of a suitable diffraction line of the reacting phase which may disappear or appear (see Fig. 2.19). Some examples are the study of phase transitions in the $CaSO_4$–H_2O system[123] and the decomposition of NH_4VO_3 (ref. 124).

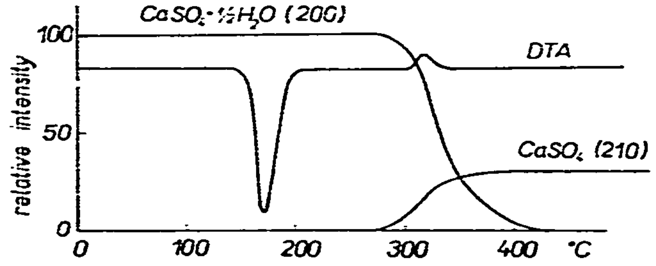

Fig. 2.19. Example of thermal X-ray analysis taken from ref. 123.

The dependence of electrical conductivity on temperature is used to detect phase transitions in *electrothermal analysis*. Although similar to dilatometry, this method makes possible the use of very low heating rates and thus approaches equilibrium conditions. It is suitable for the study of transitions in one component systems such as CaO (ref. 125), $KNbO_4$ (ref. 126), $LiNO_3$ (ref. 127), $NaNO_3$ (ref. 127) and phenanthrene[128], as well as in two component systems such as Li_2SO_4–Na_2SO_4 (ref. 129), ZrO_2–CaO (ref. 130), Ag_2SO_4–$CaSO_4$ (ref. 131). Chemical reactions are also studied by this technique[132,133]. According to Bergstein[134] the measurement of the dielectric constant as a function of temperature presents a possible and useful variation of this method, as for example in the synthesis of ferroelectric materials[134–136] (Fig. 2.20).

Magnetic Thermal Analysis is useful for Curie point determinations. An automatic balance is used to record magnetization (change of sample weight in the magnetic field applied) against temperature. Typical curves for Ni, Fe_3O_4 and Fe_3C (ref. 137) are shown in Fig. 2.21. Some solid–solid transformations may also be accompanied by a change of ferromagnetic behavior of a system, for example, the

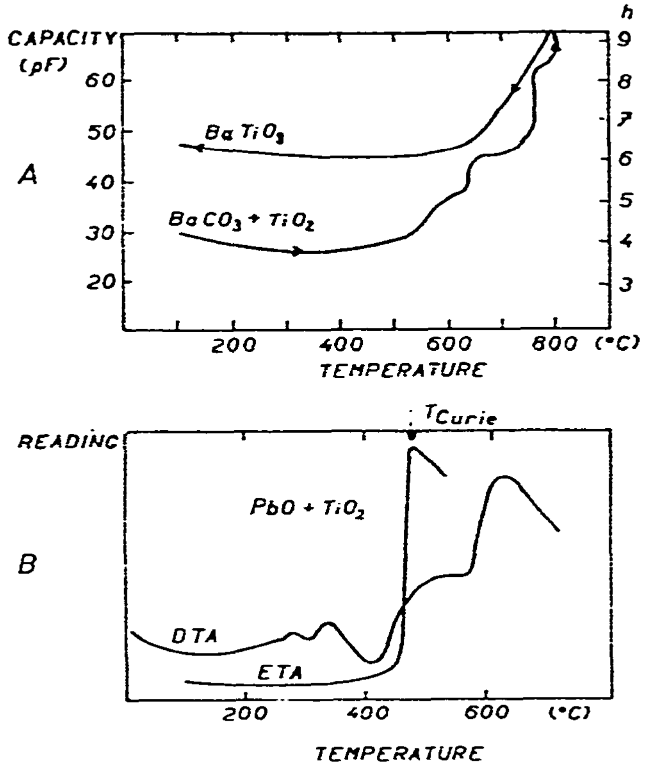

Fig. 2.20. Dielectric thermal analysis (heating rate 10 °C/min, frequency 1 MHz). A, reaction of equimolar mixture of $BaCO_3$ and TiO_2 (ref. 134) above the Curie temperature of $BaTiO_3$; B, reaction of equimolar mixture of PbO and TiO_2 (ref. 136) in comparison with DTA. The capacity maximum indicates the formation of $PbTiO_3$.

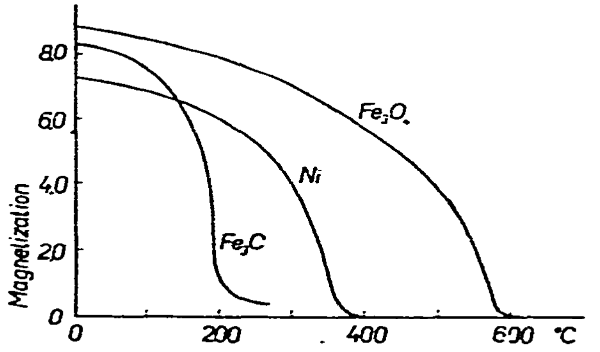

Fig. 2.21. Magnetic thermal analysis taken from ref. 137.

γ-$Fe_2O_3 \rightarrow \alpha$-$Fe_2O_3$ transition[137,138]. This method is equally successful in studying more complex processes such as Fe_3O_4 formation[139] and carbide decomposition[140,141].

Direct Thermal Analysis provides the most classical method of thermal analysis. It is based on the detection of temperature against time[142] and is suitable for processes which proceed relatively fast in comparison with the selected heating rate.

Two cases of TA curves are shown in Fig. 2.22 for slow (silicates) and fast (metals) processes of melt crystallization. It is evident that for the case of a slow process, the TA method is not sensitive enough to follow the process of crystallization. With a decreasing rate of heating (cooling) the sensitivity of the TA method is lowered due to heat transfer to the sample surroundings and thus, in most cases, it is necessary to find the optimum cooling rate with regard to the rate of the process investigated.

The theory of this technique was first given by White[143] and later by Smit[144]. For certain measurements, viz. the determination of solidus curves, the plots obtained under heating are more favorable[151] than those obtained under cooling. However, heat treatment at a temperature just below the equilibrium temperature of the transition is often required. Owing to the low temperature conductivity of some materials (such as oxides) a distinct temperature gradient is created which may distort the TA measurement. Diminishing of sample load or decreasing the sample layer is of assistance in removing this effect. This effect, together with consequent local supercooling, may result in curve hysteresis if we compare the cooling and the heating curves (see Fig. 2.23). Similar experimental conditions must be fulfilled for the study of multiple-component systems. From a suitable series of cooling curves, a nearly complete phase diagram may be constructed, as is demonstrated in Fig. 2.24. The breaks on the curve indicate the temperatures of the phase transitions while the duration of time lags correspond to the size of the heat effects. From the curve breaks, the liquidus temperatures may also be obtained. Plotting of the length of each time lag against the composition makes it possible to find the eutectic composition and/or the solid–solid transformation.

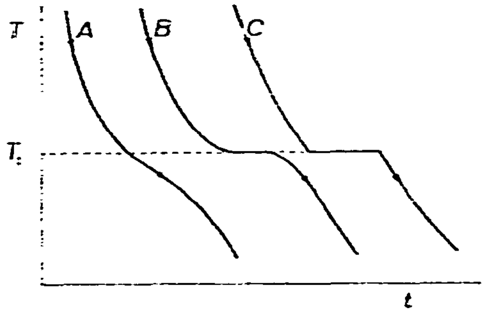

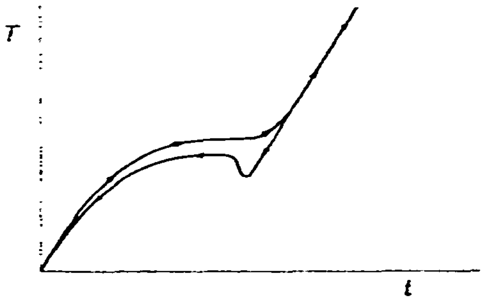

Fig. 2.22 (left). Direct thermal analysis curves for a low rate (A), fast rate (B), and idealized processes (C)

Fig. 2.23 (right). Thermal analysis hysteresis curve.

The scanning of individual points from a TA curve may not be unambiguous, and a derivative curve may sometimes be very useful. Such a DTA-like curve of the electronically generated derivative is demonstrated in Fig. 2.25 and is compared with the experimentally detected input signal of a normal TA curve. Utilization of a single thermocouple–sample system has some advantages over the ordinary DTA "twin" arrangement. Despite the fact that the mathematical description seems to be simpler than that for DTA, the theory has not been developed as yet. The use of this promising

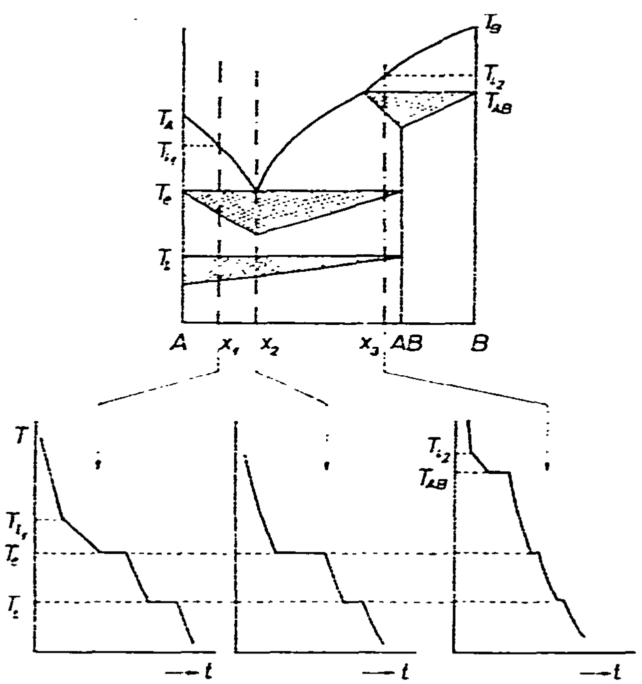

Fig. 2.24. Construction of binary phase diagram from thermal analysis measurements.

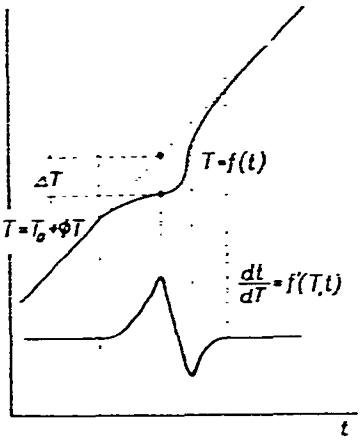

Fig. 2.25. Use of derivative curves in thermal analysis.

method is delayed due to instrumental difficulties which permit, only for the time being, a heating rate that is not less than 12°C/min. A similar method was proposed by Sze and Meaden[192] where the sample acts as its own reference.

Differential Thermal Analysis. Since most phase transitions are associated with a particular heat effect they can be preferably detected by means of DTA[63]. The difficulty connected with the interpretation of the results, as already discussed in preceding sections, is in the determination of the equilibrium temperature. If no temperature gradient is present in the sample, the sharp edge of the peak is, in this

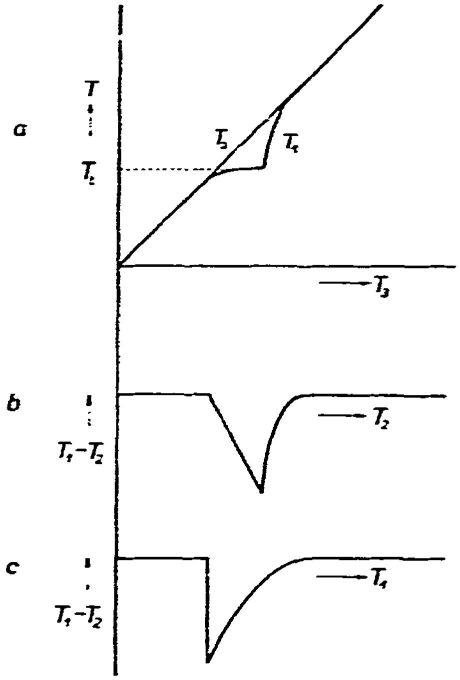

Fig. 2.26. Principle of DTA measurement; T_1, T_2, T_3 are the sample, standard, and block temperatures, respectively.

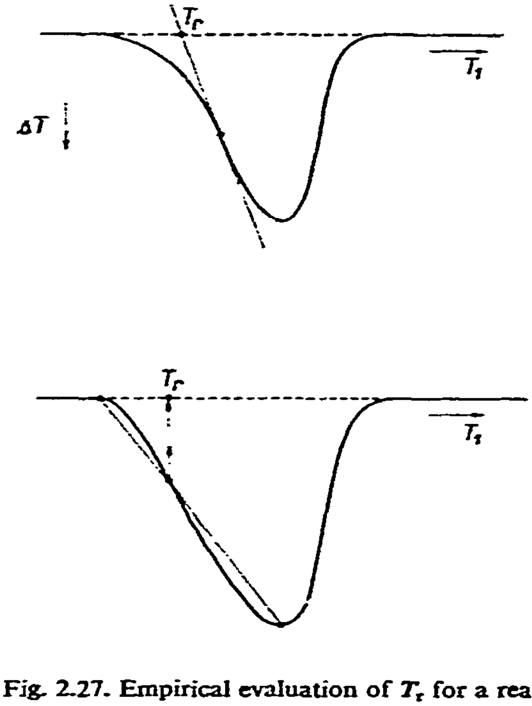

Fig. 2.27. Empirical evaluation of T_r for a reaction.

desirable and highly idealized case, identified with the equilibrium temperature of an invariant process (Fig. 2.26). For solid-state systems the temperature gradient distorts the DTA peak and due to superheating or undercooling, the whole curve may be shifted. In such cases, the edge temperature of the DTA peak is not the true equilibrium temperature. In order to overcome these difficulties different methods have been suggested such as calibration, calculation of this difference from characteristic quantities[145] and/or use of different geometrical constructions to analyze the DTA peak. However, none of these methods is completely satisfactory. Keavney and Eberlin[146] approached the process temperature determination by drawing a secant line through the points of departure from the baseline, inflection point, and the top of the peak (see Fig. 2.27). Perron et al.[147] determined this temperature at the point of intersection of the baseline with the tangent put through the inflection point, which is in accordance with the recommendations of the I.C.T.A. Standardization Committee. Hrubý[150] has successfully applied the tangent method to evaluate the glass-forming tendency[167] of semiconducting glasses by comparing their DTA peaks of transformation, crystallization and melting, as shown in Fig. 2.28.

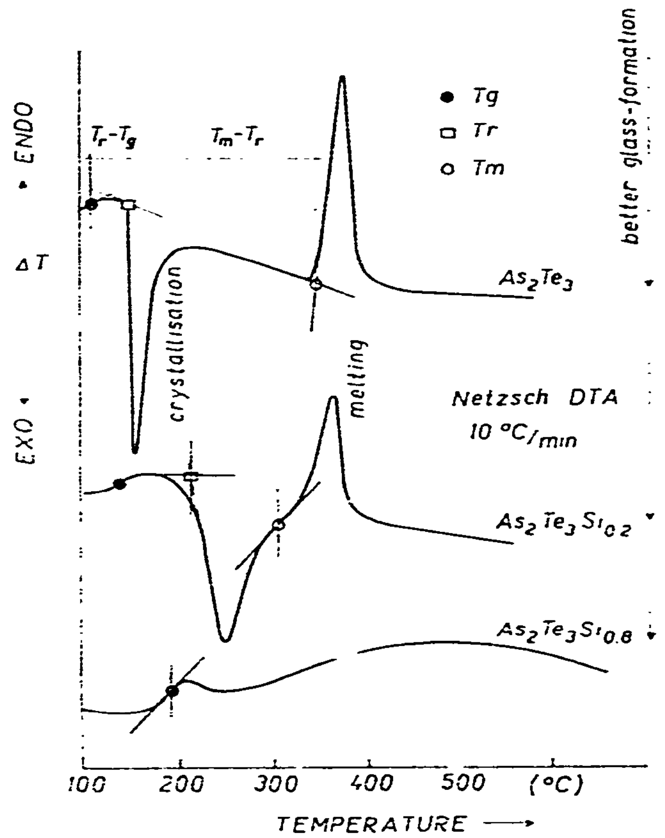

Fig. 2.28. DTA, taken from ref. 150, of glassy As$_2$Te$_3$, pure and mixtures with silica; bulk samples of 1 g in sealed quartz ampoules. According to Hrubý[150] the glass-forming tendency is given by ratio $(T_r - T_g)/(T_m - T_r)$ where T_g, T_r and T_m are the temperatures of glass transition, crystallization and melting, respectively.

The tendency to decrease the temperature gradient in the sample suggests the use of DDC or even DSC, or at least to greatly decrease the sample mass. This latter method was successfully used by Mazieres[148,149] who employed the thermocouple junction directly as a micro sample holder. The sample mass inside such a temperature sensing element was as low as 1 μg. Unfortunately, one of the problems encountered was how to clean the tiny sample container and also how to weight the sample. The theory of micro-DTA with a sandwich-type sample was recently given by Akiyama[193]. Errors arising from superheating are less frequently encountered than those caused by undercooling and hence heating rather than cooling curves are recommended[151] to investigate equilibria in condensed systems. The interpretation of such DTA curves is shown in Fig. 2.29; for details see Wunderlich[194]. For the determination of equilibrium temperatures of reversible reactions, it is convenient to study the process during both cooling and heating. The equilibrium temperature is then represented as a mean value from both measurements (see Fig. 2.30), as shown by Pöyhönen and Mansikka[152]. This method provides only approximate data because the undercooling and respective superheating may prevail during only one of these temperature modes. The advantages of Maziere's and Pöyhönen-Mansikka's methods together

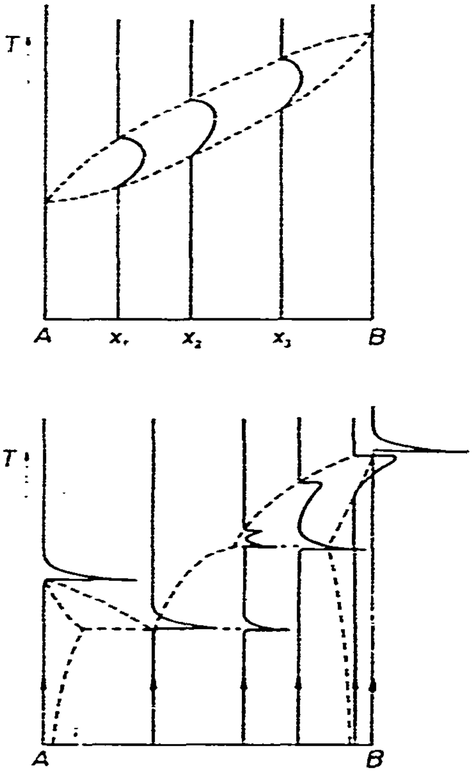

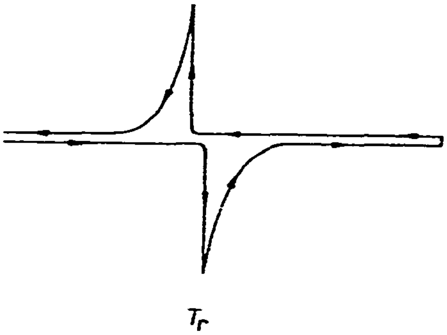

Fig. 2.29 (left). Construction of binary phase diagrams from DTA heating curves[151].
Fig. 2.30 (right). Evaluation of equilibrium temperature from heating and cooling curves.

with the removal of nucleation processes are employed in the *periodic thermal analysis* technique described by Proks[153,154]. It is based on Ordway's work[155] who first employed the thermocouple junction directly as a sample-holder, a temperature sensing element, and a high-frequency heater (it is sometimes combined with the direct observation of the sample by means of high-temperature microscopy). If the system which is composed of liquid and solid phases is considered at the equilibrium temperature, T_{eq}, and if the temperature oscillates by a certain small difference, ΔT, from T_{eq}, then, provided the periods are short enough, none of these phases disappears completely. Under such conditions, nucleation, superheating, and undercooling phenomena are not present to any extent. In addition, owing to the small sample mass there is only a small temperature gradient between the temperature measured and the actual temperature in the sample and the equilibrium temperature falls within the maximum and minimum sample temperature range. The thermocouple junction is heated by a high-frequency current modulated by a low-frequency component of a suitable time period (preferably simple sinusoidal signal with 1–10 Hz frequency). A coupled oscilloscope serves to register the dependence of T, as shown by the equation

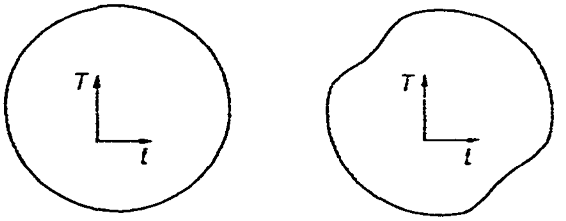

Fig. 2.31. Typical curves for periodic thermal analysis[154].

$$-\mathrm{d}T/\mathrm{d}t = \mathrm{f}_1(T) \tag{2.69}$$

The temperature-dependent signal may lead to the vertical oscilloscope input against a suitable time base, or

$$T = \mathrm{f}_2(t) \tag{2.70}$$

as shown in Fig. 2.31. The oscillogram is circular only in the case where no processes occur in the thermocouple junction. During fusion and solidification processes the circle is deformed in parts where melting and crystallization take place.

The advantage of *differential scanning calorimetry* over DTA is the better reproducibility of the temperature measurement of phase transformations. The simplest case, utilized by Gray[59] and David[61] (section 2.2.4), is the assumption that the sample and the sample holder have much higher thermal conductivities than the interfacial region so that the temperature gradient is confined to the latter region. Due to the small ratio of sample mass to that of the holder, thermal effects taking place in the sample do not perturb the sample-holder [156,157]. A number of other

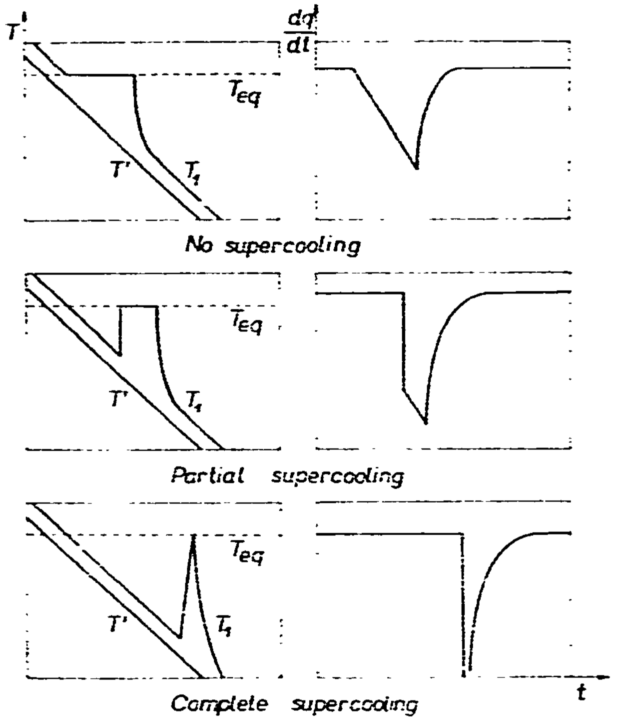

Fig. 2.32. Effect of undercooling on the shape of the TA and the DSC curves (according to Flynn[157]).

model cases have been assumed; for example, according to Flynn[156], idealized temperature vs time and dq/dt vs time curves, as shown in Fig. 2.32, where T_1, T' and T_{eq} are the temperatures of the sample, its holder and the sample fusion respectively, under a constant heating rate, ϕ. If partial or complete supercooling takes place, as in the middle and lower curve of Fig. 2.32, there appears a sudden jump in dq/dt, followed by the usual decay. All of these idealized curves approximately duplicate curves obtained by DSC for the cooling (and heating) of pure elements and compounds. According to Flynn[156], the extrapolated onset temperature, T_0, is related to the actual temperature, T_{eq}, by the equation

$$T_0 = T_{eq} + \phi(\tau_T + \tau_X + \tau_S) \tag{2.71}$$

where τ_T is the temperature programming constant, τ_X is the differential power time constant and τ_S $(= C_{p1} m_1 - C_p' m')/K'A')$ is the time decay constant proportional to interfacial conductivity K' between the sample (1) and its holder ('). Symbols C_p, m and ϕ are the specific heat, the mass, and the heating rate, respectively, and A' is the contact area between the sample and its holder. The precision of the temperature calibration is reported to be dependent on the experimental reproducibility of the interfacial time constant, τ_S, since the instrumental time constants, τ_T and τ_X, do not change. For a calorimetric measurement, the dependence of dq/dt vs. t is recorded; for a temperature determination, a plot of dq/dt vs. T is preferable. The recorded difference is illustrated for the melting of zinc in Fig. 2.33.

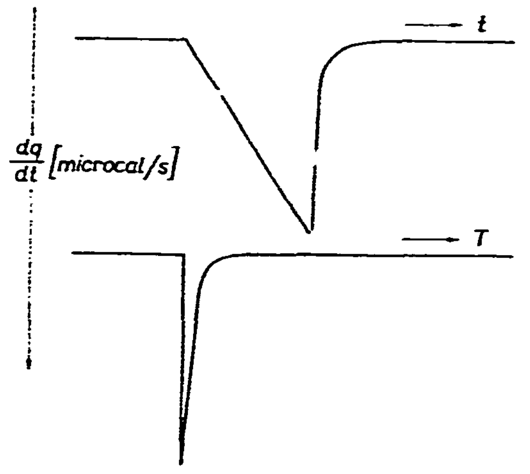

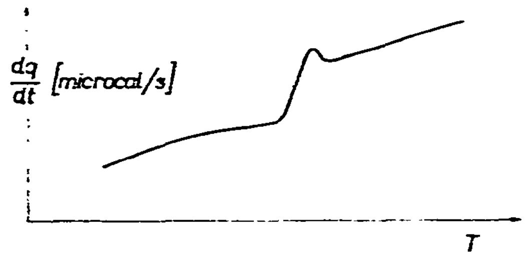

Fig. 2.33 (left). DSC curves for a first order transition related to time (t) or temperature (T).
Fig. 2.34 (right). DSC curve for a glass transition.

This method is suitable for the determination of transition of metastable (frozen in) modifications such as in metastable glutaronitrile at 233K, the existence of which was determined[158]. Well defined applicability is found in the determination of the temperature of glass transformations[159] (see Fig. 2.34) and other second order transitions. Another use may be shown by order–mesophase transitions of some organic compounds interpreted on C_p–T diagrams[160].

Permeability thermal analysis, which was introduced by Komrska[191] to follow sintering processes, is also suitable to study the thermal decomposition of solids. The principle of this method is the continual gas-permeability measurement of a porous sample under its programmed heating. Since the sintering process is associated with the decreasing permeability, the decomposition exhibits a sudden increase of apparent permeability due to gas evolution.

Although the *combined methods* hold some advantages, particularly in a preliminary, analytical description of a sample, they are seldom of use in the specialized physico-chemical investigations. The individual techniques require characteristic process determining experimental modes compatible only with the particular method. The combined methods may well serve for the first approach to an unknown system where the nature and the region of the processes is to be defined. There has been no attempt made here to give a complete enumeration of all of the methods and their applicability, but it should be pointed out that methods such as high-temperature reflectance spectrometry and/or spectrophotometry etc., are also of great value.

2.4.2. Methods for the study of solid–gas equilibria

As typical cases, the following processes, $A_{(s)} \rightleftarrows A_{(g)}$ and/or $AB_{(s)} \rightleftarrows A_{(s)} + B_{(g)}$ will be considered. According to the phase rule, two phases in a one component system and three phases in a two component system are invariant. In pure condensed systems (section 2.4.1) the influence of pressure is neglected. However, if gases participate in the process the equilibrium temperature becomes very sensitive to pressure and hence the pressure cannot be neglected. The pressure–temperature relationship involving the vaporization of pure solids cannot be determined by visual observations and evolved gas techniques are useful. The quality of equilibrium data measured depends on the methods described in section 2.4.1, on the accuracy and the correctness of the temperature detection, and also on securing the constancy of defined pressure conditions on the solid–gas interface. The assertion of a predefined pressure to be held constant during a reaction has some experimental complications for DTA, DSC and TG, where a given sample is surrounded by a static atmosphere or is in a gas stream. Such a dynamic atmosphere provides certain hydrodynamic conditions controlling the entire contact area between the gas and the reacting solid surface. A better defined pressure condition can be attained in flow systems[161] where the gaseous product is analyzed to determine the propagation of the process. It is necessary to achieve minimum delay between the sensing temperature and the fractional decomposition. Correct temperature measurement also presents experimental difficulties. The requirement to have the temperature-sensing element directly in the system investigated, or more accurately, in the phase boundary where the process takes place, is almost unattainable particularly in TG investigations. Such a temperature gradient may cause a substantial error. This may be removed by using two geometrically similar cells, one as a sample-holder suspended from the thermobalance holder, and the other as a temperature sensing cell placed underneath the first one in a symmetrically heated chamber, as shown by Šesták[162]. In pure condensed systems, there is a shift in the transition temperature due to undercooling and superheating phenomena. For reversible processes, it is desirable to follow the decomposition advance at an increasing temperature while in recombination processes it is better to detect it at a decreasing temperature. The preferred method for this appears to be DTA[153,154] because during a process a constant number of phases is maintained.

The DTA method was applied to the study of sublimation equilibria by Meyer et al.[163] for the systems: NH_4Cl, NH_4Br and NH_4I at atmospheric pressures. The temperatures, T_{exp}, scanned from the DTA curves, (Fig. 2.35) are in a good agreement with the literature data for atmospheric pressure sublimation temperatures, T_{lit}. They are compared in the following table:

TABLE 2.3

SUBLIMATION TEMPERATURES OBTAINED FROM DYNAMIC MEASUREMENTS (T_{exp}) AND STATIC EQUILIBRIUM MEASUREMENTS (T_{lit})

Substance	T_{exp}	T_{lit}
NH_4Cl	338.2	337.8
NH_4Br	395.2	394.6
NH_4I	403.6	404.0

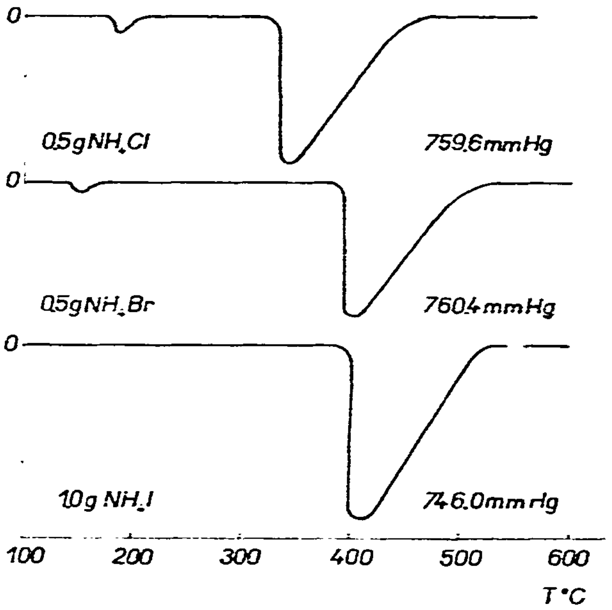

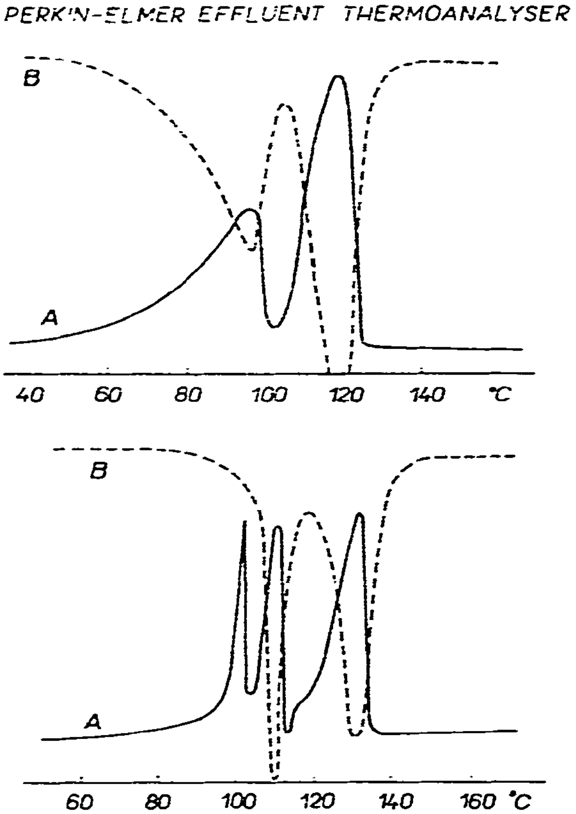

Fig. 2.35. Determination of sublimation temperatures from DTA curves.

Fig. 2.36. Effect of sample arrangement on the shape of a DTA[167] curve (A), and evolved gas detection curve (B). Upper part exhibits curves for open sample pan; bottom curves for sample pan with pin hole.

By comparing the DTA results for a series of different pressures, the dependence of the sublimation temperature on pressure can be established. There was a good agreement with the literature data obtained using the static method as reported by Smith and Calvert[164] for NH_4Cl.

For investigations carried out by DSC, a pin-holed lid placed on the top of the sample holder is recommended so that the evolved gases can escape. The resulting peaks are much sharper and thus the accuracy of temperature measurement is greater. The curves for the dehydration of $CuSO_4 \cdot 5H_2O$ obtained under atmospheric pressure in an open sample-holder (a) and in a pin-holed lid (b) are compared in Fig. 2.36. The combination of calorimetric measurements with the simultaneous analysis of gaseous products[165] (see Fig. 2.36 dashed lines) is very useful. From a comparison of curve (a) and (b), it is evident that the first peak corresponds to the internal transformation which does not involve the loss of water. These simultaneous techniques have been used also in combination with DTA in the $BaCl_2$–H_2O system[166]. For details, see Schultze[167].

The works of Wendlandt et al.[168,169], who used complementary measurements of magnetic susceptibility, thermal conductivity, TG and DTA to study the deaquation of the cobalt halide hydrate, and of Bergstein et al.[134–136,170,171] who investigated solid–gas reactions in the spinel and perowskite formation by DTA, TG, dilatometry, X-ray and thermoelectrical measurements, can serve as examples of the successful application of the complex method of thermal analyses. As in the case of derivative curves in TA, a similar arrangement can be used for DTA (DDTA) and TG (DTG) measurements as well. In Fig. 2.37, TG and DTG curves for the reduction of α-$Fe_2O_3 \cdot H_2O$ in hydrogen are shown. The increase in resolving power of the derivative curve electronically obtained against a weight loss curve is evident.

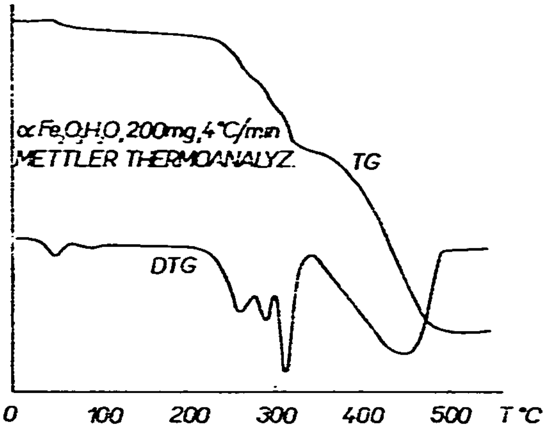

Fig. 2.37. Typical TG and DTG curves.

2.4.3. *Methods for the study of liquid–gas equilibria*

The normal boiling point is defined as the temperature at which the equilibrium vapor pressure is one atmosphere. In an open system, the rate of such a liquid–vapor transition is controlled by the rate at which the vapor is removed from the region of the liquid–vapor interface. The shape of a DTA and/or DSC curve is determined by

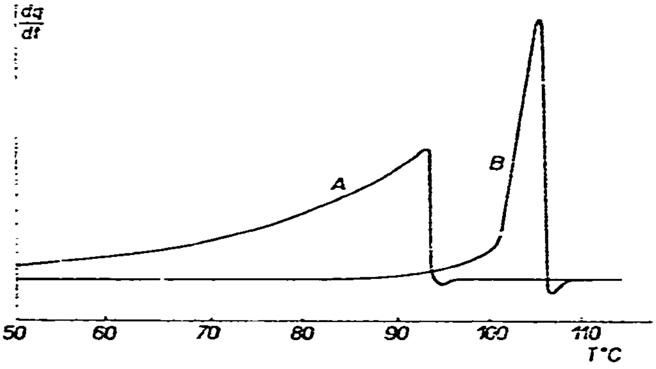

Fig. 2.38. DSC curves for evaporation of water. Curve A, open sample pan; curve B, sample pan with pin hole.

the rate of vaporization as a function of temperature which, in turn, is affected by the rate at which the vapor is removed. The surface area of the liquid and the size of the orifice through which the vapor escapes to the surroundings are the important factors. Because the liquid is enclosed in a rather deep container in ordinary DTA experiments, the evaporation takes place close to the normal boiling point. At this point the vapor is forced from the cavity under a positive pressure and thus a sharp peak is produced. The best procedure for boiling point determinations is to use the DSC method provided that the sample container limits the rate of vaporization. This again may be accomplished by using a sample pan containing a pin-hole in its cover. The vaporization peak of water under these conditions is shown in Fig. 2.38. The heat of vaporization at the boiling point can also be obtained from the peak area but, for an accurate measurement, the correction for sample loss up to the point where the peak begins must be made. Paulik et al.[172] used a microdistillation method for the boiling point determination where the weight loss versus temperature was recorded. Precise determination of melting and boiling points has recently been discussed by Barrall[195].

2.5. Calculation of the standard enthalpy change of phase transitions from phase diagrams

The condition of two phases in equilibrium is expressed by the Clausius–Clapeyron equation (see Chapter 1), or

$$\frac{\mathrm{d}P}{\mathrm{d}T} = \frac{\Delta H}{T\Delta V}. \tag{2.72}$$

The direct experimental investigation of the dependence of the equilibrium pressure upon the temperature enables the calculation of ΔH and/or ΔV quantities. In condensed systems such a dependence can be established by DTA (fusion, modification transformation, etc.). If the quantity, ΔV, is determined at the same time using density (ρ) measurements of both phases ($V_i = 1/\rho_i$), then ΔH may be calculated provided that it is temperature independent in the narrow temperature interval. If P_1 relates to temperature, T_1, and P_2 to T_2, then the integrated form of eqn. (2.72) is

$$\Delta H = \frac{\Delta V(P_2 - P_1)}{\ln (T_2/T_1)}. \tag{2.73}$$

This method was successfully applied to determine the standard change of enthalpy for the transformations: cristoballite → quartz[173]; solid–solid transformation of CsCl[174]; and others (NH_4Cl, NH_4NO_3, Na_3AlF_6, CeO_2, etc.)[175]. Pressures up to 1500 atm. were employed.

The enthalpy change which accompanies first order transitions can also be determined from a binary phase diagram obtained by any TA method. For a phase diagram where the components do not form a solid solution, the heat of fusion for individual components may be obtained from the course of the liquidus curve in the vicinity of the fusion temperature of the pure component assuming ideal behavior of the liquid solution. On integration of eqn. (1.38), under the assumption that the enthalpy change is temperature independent

$$\ln x_A = -\frac{\Delta H_A}{R}\left(\frac{1}{T}-\frac{1}{T_A}\right). \tag{2.74}$$

By plotting $\ln x_A$ versus $1/T$ a straight line is obtained the slope of which gives ΔH_{fusion} of component A. A series of such established data are reported by Kelley[176]. A typical example of the calculation may be found in the work of Bowen[177] for the system, Na_2SiO_3–SiO_2 (including determination of $\Delta S_A = \Delta H_A/T_A$).

If the specific heats of the pure liquid and solid components are known as a function of temperature, such as by the empirical equation

$$C_p = a + bT + cT^{-2}$$

where a, b and c are constants, the ΔH_A may be expressed using the integrated form of eqn. (1.38), or

$$\begin{aligned} R\ln x_A = {} & -\Delta H_A\left(\frac{1}{T}-\frac{1}{T_A}\right) - \Delta a\left(\frac{T_A}{T} + \ln\frac{T}{T_A} - 1\right) + \\ & + \Delta b\left[T - T_A + T_A^2\left(\frac{1}{T}-\frac{1}{T_A}\right)\right] + \\ & + \Delta c\left[2\left(\frac{1}{T^2}-\frac{1}{T_A^2}\right) - \left(\frac{1}{T_A T}-\frac{1}{T_A^2}\right)\right]. \end{aligned} \tag{2.75}$$

The terms, T_A and T, are the temperatures of fusion and of the system, respectively; ΔH_A is the standard enthalpy change of fusion at the temperature T_A; and x_A is the molar fraction of the component A. Practical application, however, is attained on using some simplification such as $T_A - T \to 0$, $\Delta b \to 0$ and $\Delta c \to 0$. A survey of the methods of ΔH calculation is given by Adams and Cohen[178].

In the case of sublimation or possibly some evaporation, the volume of the condensed phase may be neglected with respect to that of the vapor ($\Delta V \cong V_g$). Assuming ideal behavior of the gaseous phase, eqn. (2.72) becomes

$$\frac{\mathrm{d}\ln p}{\mathrm{d}T} = \frac{\Delta H}{RT^2}. \tag{2.76}$$

Considering ΔH as temperature independent, the integration yields

$$\ln p = -\frac{\Delta \bar{H}}{RT_{eq}} + \text{const.} \tag{2.77}$$

A plot of T_{eq} against p, or $1/T_{eq}$ against $\ln p$ established experimentally by DTA, DSC, TG, etc., provides the necessary data to calculate $\Delta \bar{H}$ which represents the mean value in the given temperature interval.

In accordance with the procedure of eqn. (2.75), known empirical dependence of the specific heat versus temperature may be assumed, or

$$-R \ln p = \frac{\Delta H}{T} - \Delta a \ln T - \frac{\Delta b}{2} T + \frac{\Delta c}{2T^2} + C_{78} \tag{2.78}$$

where C_{78} is the integration constant. Upon rearrangement,

$$\sum = -R \ln p + \Delta a \ln T + \frac{\Delta b}{2} T - \frac{\Delta c}{2T^2} = \frac{\Delta H}{T} + C_{78} \tag{2.79}$$

A plot of the left-hand side of eqn. (2.79) ($\sum$) against the reciprocal temperature, $1/T$, gives a straight line with a slope equal to the enthalpy change corresponding to the phase transition at the temperature of equilibrium.

Many organic vapors, however, with different intermolecular and intramolecular attractions may deviate considerably from the ideal gas behavior assumed by eqn. (2.76). Corrected equations have been proposed to calculate the change in volume ($V = ((1-P)T_r)^{1/2}$, where $T_r = T/T_{\text{critical}}$ = reduced temperature) and/or the vapor pressure function ($\log P = a - b/(c+T)$ where a, b and c are constants) and combined with the Clausius–Clapeyron equation, such as described by Morie et al.[179].

Similar relations may be used if sublimation is associated with a chemical reaction. From eqn. (1.54) it follows that

$$\left(\frac{\partial \ln K}{\partial T}\right)_P = \frac{\Delta H^\circ}{RT^2} \tag{2.80}$$

The process of $A_{(s)} \rightleftharpoons B_{(g)} + C_{(s)}$, where the components A and C do not form a solid solution, is then described as

$$\left(\frac{\partial \ln p}{\partial T}\right)_P = \frac{\Delta H^\circ}{RT^2}. \tag{2.81}$$

As an example, the work of Markowitz and Boryta[180] on the sublimation equilibria of NH_4Cl, NH_4I and NH_4Br by DTA may be mentioned. It is known that ammonium halides are completely dissociated in the vapor phase ($NH_4X_{(s)} \rightleftharpoons NH_{3(g)} + HX_{(g)}$). Accordingly, the vaporization of NH_4Cl represents a dissociation process for which the standard free energy change can be readily computed from the experimental sublimation pressures, or

$$\Delta G^\circ_{\text{diss}} = -RT \ln K_p = -RT \ln (p_{NH_3}\, p_{HCl}) = -RT \ln \frac{P^2}{4} \tag{2.82}$$

where P refers to the sublimation pressure of amonium chloride ($P = 2p_{HCl} = 2p_{NH_3}$). Then

$$\frac{d \ln K_p}{dT} = \frac{2d \ln P}{dT} = \frac{\overline{\Delta H^\circ_{\text{diss}}}}{RT^2} = \frac{2\overline{\Delta H^\circ_{\text{subl}}}}{RT^2}. \tag{2.83}$$

From a plot of ln P against $(1/T)$ the slope, $-\overline{\Delta H^{\circ}_{subl}}/R$, is obtained, where $\overline{\Delta H^{\circ}_{subl}}$ is the average value of the enthalpy of sublimation over the temperature range covered. Similarly, Stone[181] and later Ellis and Mortland[182] applied eqn. (2.82) to determine the reaction enthalpy of $MgCO_{3(s)} \rightleftharpoons MgO_{(s)} + CO_{2(g)}$ from the dependence of the temperature of magnesite decomposition on the partial pressure of carbon dioxide. The accuracy of the results obtained is of the same degree as the accuracy of the peak area measurement. Analogous determinations for $NiCO_3$ and $CaCO_3$ were made by Buzdov[183]. A variety of authors used this method for standard reaction enthalpy determinations such as for kaolinite[182], $BaCl_2{\cdot}2H_2O$ (ref. 184), $MgSO_4{\cdot}7H_2O$ (ref. 186), $Mg(OH)_2$ (ref. 189) and others[185–188].

REFERENCES

1 J. Velíšek, *Czech. J. Phys.*, A 20 (1970) 513.
2 P. D. Garn, *Thermoanalytical Methods of Investigation*, Academic Press, New York, 1965.
3 D. Schultze, *Differentialthermoanalyse*, VEB Deutscher Verlag der Wissenschaften, Berlin, 1969.
4 Perron and Mathieu, *Chim. Anal. (Paris)*, 46 (1964) 293.
5 W. W. Wendlandt, *Thermal Methods of Analysis*, Wiley, New York, 1964.
6 L. G. Berg, *Vvedenie v termografiju*, I.A.N. SSSR, Moskva 1961.
7 G. O. Pilojan, *Vvedenie v téoriu termičeskogo analyza*, I.A.N. SSSR, Moskva, 1965.
8 W. J. Smothers and Y. Chiang, *Handbook of Differential Thermal Analysis*, Chem. Publ. Co., New York, 1966.
9 J. Šesták and G. Berggren, *Chem. Listy*, 64 (1970) 695.
10 R. L. Bohon in H. G. McAdie (editor), *Proc. 1st, Toronto Symp. Therm. Anal., CIC, Canada*, 1965, p. 63.
11 A. Gäumann and J. Oswald, *Chimia*, 21 (1967) 421.
12 W. Leegscheider, *Ber. Bunsenges. Phys. Chem.*, 71 (1967) 228.
13 K. Heide, *Silikattechnik*, 17 (1966) 447.
14 G. Berggren, *Proceedings of 1st Scandinavian Symp. Thermal Anal., by Nordforsk, Helsinki (1971)*.
15 M. J. Vold, *Anal. Chem.*, 21 (1949) 683.
16 P. F. Kerr and J. L. Kulp, *Amer. Miner.*, 33 (1948) 387.
17 H. J. Borchardt and F. Daniels, *J. Amer. Chem. Soc.*, 79 (1957) 41; and H. J. Borchardt, *J. Chem. Educ.*, 33 (1956) 103.
18 J. J. Kessis, *C.R. Acad. Sci.*, C270 (1970) 1; C270 (1970) 121; C270 (1970) 265; C270 (1970) 1201.
19 J. Proks, *Silikaty*, 5 (1961) 114.
20 G. Adam and F. H. Müller, *Kolloid. Z. Z. Polym.*, 192 (1963) 29.
21 S. L. Boersma, *J. Amer. Ceram. Soc.*, 38 (1955) 281.
22 H. T. Smyth, *J. Amer. Ceram. Soc.*, 34 (1951) 221.
23 J. L. Soulé, *J. Phys. Radium*, 13 (1951) 221.
24 E. Erickson, *Amer. Royal Agr. College Sweden*, 19 (1952) 127; *ibid.*, 20 (1953) 117; E. Kunge: *Lantbrukshögsholans Annaler*, 21 (1955) 189.
25 G. M. Lukaszewski, *Lab. Pract.*, 14 (1965) 1277; 14 (1965) 1399; 15 (1966) 82; 15 (1966) 187; 15 (1966) 302; 15 (1966) 431; 15 (1966) 551; 15 (1966) 664; 15 (1966) 762; 15 (1966) 861.
26 L. G. Berg and V. P. Egunov, *J. Thermal Anal.*, 1 (1969) 5.
27 E. Deeg, *Ber. Deut. Chem. Ges.*, 10 (1956) 321.
28 A. A. Blumberg, *J. Phys. Chem.*, 63 (1959) 1129.
29 A. A. Blumberg and S. C. Stavrinov, *J. Phys. Chem.*, 64 (1960) 1438.
30 E. B. Allison, *Clay Miner. Bull.*, 2 (1955) 242.
31 Y. Tzusuki and K. Nagasawa, *J.E.S. Nagoya Univ.*, 5 (1957) 153.
32 R. Melling, F. W. Wilburn and R. M. MacIntosh, *Anal. Chem.*, 41 (1969) 1275.
33 E. M. Barrall II and L. B. Rogers, *Anal. Chem.*, 34 (1962) 1101.
34 I. Barshad, *Amer. Mineral.*, 37 (1952) 667.
35 B. Jankovski, *Silikattechnik*, 17 (1966) 22.

36 G. de Jong, *J. Amer. Ceram. Soc.*, 40 (1957) 42.
37 H. S. Carslaw and J. C. Jaeger, *Conduction of Heat in Solids*, Clarendon Press, Oxford, 1959.
38 P. Pacor, *Anal. Chim. Acta*, 37 (1967) 200.
39 A. G. Merzkanov, N. I. Durakov, N. P. Ikrijanikov and L. T. Abramova, *Zh. Fiz. Khim.*, 40 (1966) 437.
40 L. G. Berg and V. P. Egunov, *Zh. Neorg. Khim.*, 14 (1969) 593.
41 W. P. Brennan, B. Miller and J. C. Whitwell, *Ind. Eng. Chem. Fundam.*, 8 (1969) 314.
42 C. Plato and A. R. Glasgow, *Anal. Chem.*, 41 (1969) 330.
43 J. A. Hedvall, R. Lindner and N. Hartler, *Acta Chem. Scand.*, 4 (1950) 1099.
44 H. G. Wiedemann and A. van Tets, *Thermochim. Acta*, 1 (1970) 159.
45 C. H. Kheite and W. Viehman, *J. Appl. Polym. Sci.*, 5 (1961) 86.
45a E. L. Dosch, *Thermochim. Acta*, 1 (1970) 367.
45b H. Svoboda and J. Šesták, *Proc. VI Czech. Conf. Thermal Anal., High Tatras, 1973*, SVŠT, Bratislava, 1973, p. P19–P32.
46 H. G. MacAdie, *Can. J. Chem.*, 40 (1962) 2195.
47 H. G. Wiedemann, *Z. Anal. Chem.*, 220 (1966) 81.
48 K. Tarkar, K. Lasser and H. P. Fritzer, *Sprechsaal*, 95 (1962) 239.
49 H. G. McAdie, in R. F. Schwenker and P. D. Garn (editors), *Thermal Analysis*, Vol. 2, Academic Press, New York, 1969, p. 1499; and Vol. 1 (see ref. 50), p. 591.
50 R. C. Mackenzie and P. F. S. Ritchie, in H. G. Wiedemann (editor), *Thermal Analysis* (*Proc. IIIrd ICTA*), Vol. 1, Birkhauser Verlag, Basel, 1972, p. 441.
51 H. E. Schwiete and G. Ziegler, *Ber. Deut. Chem. Ges.*, 35 (1958) 193.
52 M. M. Faktor and R. Hanks, *Trans. Faraday Soc.*, 63 (1967) 1122.
53 L. Eyraud, *C.R. Acad. Sci.*, 238 (1954) 1511.
54 L. Eyraud and J. L. Petit, *Chim. Mod.*, 6 (1961) 141.
55 D. M. Speros and R. L. Woodhouse, *J. Phys. Chem.*, 72 (1968) 2846; 67 (1963) 2164.
56 E. S. Watson, M. J. O'Neil, J. Justin and N. Brenner, *Anal. Chem.*, 36 (1964) 1233.
57 R. A. Baxter, in R. F. Schwenker and P. D. Garn (editors), *Thermal Analysis*, Vol. 1, Academic Press, New York, 1969, p. 65.
58 M. J. O'Neil, *Anal. Chem.*, 38 (1966) 1331.
59 A. P. Gray, lecture at *The IIIrd ICTA, Davos, Switzerland, 1971.*
60 M. J. O'Neil and A. P. Gray, in H. G. Wiedemann (editor), *Thermal Analysis* (*Proc. IIIrd ICTA*), Vol. 1, Birkhäuser Verlag, Basel, 1972, p. 279.
61 D. J. David, *J. Thermal Anal.*, 3 (1971) 247.
62 A. P. Gray, in R. J. Porter and J. F. Johnson (editors), *Analytical Calorimetry*, Vol. 1, Plenum Press, New York, 1968, p. 209.
63 P. D. Garn, *Anal. Chem.*, 41 (1969) 447.
64 D. S. Nicholson and R. M. Fulrath, *J. Amer. Ceram. Soc.*, 53 (1970) 237.
65 E. Murrill and L. Breed, *Thermochim. Acta*, 1 (1970) 239.
66 R. E. Farritor and L. C. Tao, *Thermochim. Acta*, 1 (1970) 297.
67 I. Mita, I. Imai and H. Kambe, *Thermochim. Acta*, 2 (1971) 337.
68 W. P. Brennan, B. Miller and J. C. Whitwell, *Thermochim. Acta*, 2 (1971) 354.
69 P. Hidnert and W. Sonder, *Thermal Expansion of Solids*, U.S. Nat. Bur. Standards, Circ. 486, (March 15, 1950).
70 W. D. Kingery, *Property Measurements at High Temperatures*, Wiley, New York, 1959.
71 R. F. Geller and P. J. Javorsky, *J. Res. Nat. Bur. Stand.*, 35 (1945) 87.
72 J. Krempasky, *Measurement of Thermophysical Properties*, Publ. House of Slovak Academy of Science Bratislava, 1969 (in Slovakian).
73 J. C. Turnbull, *J. Amer. Ceram. Soc.*, 33 (1950) 54.
74 M. L. Dannis, *J. Appl. Polym. Sci.*, 4 (1960) 249.
75 F. C. Nix and D. MacNair, *Rev. Sci. Instrum.*, 12 (1941) 66.
76 J. D. Hauswalt and L. K. Frevel, *Z. Kristallogr.*, 98 (1937) 84.
77 J. Vlnatý, *Thermochim. Acta*, 2 (1971) 163.
78 J. Gillod, *Verres Refract.*, 3 (1949) 217.
79 R. G. Loasby, *J. Sci. Instrum.*, 38 (1961) 306.
80 *Metody izměrenija těplovogo rozširenija stěkol i splaivajenych s nimi metalov* (Sbornik symposia – Leningrad July 1966), Izdat. Nauka, Leningrad, 1967.

81 A. Reiss, *Z. Phys.*, 1 (1920) 204.

82 H. Chikara and S. Seki, *Nature*, 162 (1948) 773.

83 R. K. Kirby, *J. Res. Natl. Bur. Stand.*, 57 (1956) 95.

84 A. Müller, *Proc. Roy. Soc. (London)*, A 178 (1941) 227.

85 E. Grüneisen, *Handbuch der Physik*, 10. (i) Springer, Berlin, 1926.

86 J. N. Eastabrook, *Phil. Mag.*, 2 (1957) 1421.

87 M. H. Schreiber and M. H. Waldman, *Can. J. Chem.*, 37 (1959) 1782.

88 W. C. McCrone, *Application of Thermal Microscopy*, Mettler Instrum. Corp., Princeton, N.J., *Tech. Inform. Bull.*, (1968) 3003.

89 H. A. Morton, *Laboratory Technique in Organic Chemistry*, McGraw-Hill, London, 1938.

90 R. H. Muller and S. T. Zenchelski, *Anal. Chem.*, 24 (1952) 844.

91 A. Furst and J. Shapiro, *Anal. Chem.*, 26 (1954) 1082.

92 H. Jucker and H. Suter, *Fortschr. Chem. Forsch.*, 11 (1969) 430.

93 A. van Tets and H. G. Wiedemann, in R. F. Schwenker and P. D. Garn (editors), *Thermal Analysis*, Academic Press, New York, 1969, Vol. 1, p. 121.

94 R. P. Miller and G. Sommer, *J. Sci. Instrum.*, 43 (1966) 293.

95 H. P. Vaughan, *Thermochim. Acta*, 1 (1970) 111.

96 T. Seiyama and N. Yamazol, *J. Cryst. Growth*, 2 (1968) 255.

97 P. I. Sell and A. W. Neumann, *Z. Phys. Chem. (Frankfurt am Main)*, 65 (1969) 13.

98 K. Heide, in H. G. Wiedemann (editor), *Thermal Analysis (Proc. IIIrd ICTA)*, Birkhäuser Verlag, Basel, 1972, Vol. 1.

99 H. P. Brückner and K. Heide, *Z. Chem.*, 10 (1970) 125.

100 V. Šatava, *Zem. Kalk Gips*, 20 (1967) 343.

101 D. R. Rees, P. N. Nordbrerg, S. P. Eriksen and J. V. Swintosky, *J. Pharm. Sci.*, 50 (1961) 177.

102 S. Chromý, *Silikaty*, 10 (1966) 338; *J. Amer. Ceram. Soc.*, 50 (1967) 677.

103 S. Chromý, *Silikaty*, (1974) in press.

104 H. J. Dichtl and E. Jeglitsch, *Radex Rundsch.*, (1967) 716.

105 I. P. Kushnir and E. I. Estrin, *Zarod. Lab.*, 34 (1968) 1131.

106 R. B. Gosman, *Properties of Silica*, Chemical Catalogue Company, New York, 1927.

107 H. Hennig, *Explosivstoffe*, 16 (1968) 169.

108 K. Gesi, *J. Phys. Chem. Japan*, 26 (1969) 953.

109 E. Rysdikewitsch, *Oxide Ceramics*, Academic Press, New York, 1960.

110 V. A. M. Brabers, *J. Phys. Chem. Solids*, 32 (1971) 2181.

111 R. Nagao, *Nippon Gomu Kyokaishi*, 41 (1968) 509; *Chem. Abs.*, 69 (1969) 7859.

112 P. Bariac, M. Murat and C. Eyraud, *Rev. Mater. Const.*, 606 (1966) 115.

113 N. Saito, *Solid State Phys.*, 14 (1963) 344.

114 S. Hamda, T. Sato and T. Shirai, *Bull. Chem. Soc. Jap.*, 41 (1968) 135.

115 R. A. Haldon and R. Simha, *J. Appl. Phys.*, 39 (1968) 1890.

116 N. Saito, *Solid State Phys.*, 14 (1963) 344.

117 P. D. Pathak, M. C. Gupta and J. M. Trivedi, *Indian J. Phys.*, 43 (1969) 104.

118 K. K. Kelley, J. C. Southart and C. T. Anderson, *Techn. Paper No. 625*, Bureau of Mines, Washington, 1944.

119 V. Balek, *J. Radioanal. Chem.*, 2 (1969) 315.

120 V. Balek, *J. Mater. Sci.*, 4 (1969) 919.

121 V. Balek, *Silikaty*, 13 (1969) 39.

122 P. F. Levy, *Laboratory*, 1 (1970) 1; and DuPont No. 941 Thermomechanical Analyzer Booklet.

123 H. Migazaki, *Sekko To Sekkai*, 99 (1969) 59.

124 M. Kato, M. Taniguchi and T. Kubo, *Kogyo Kagaku Zasshi*, 69 (1966) 2102.

125 J. B. MacChesney and H. J. Guggenheim, *J. Phys. Chem. Solids*, 30 (1969) 225.

126 P. D. Garn and S. Flaschen, *Anal. Chem.*, 29 (1967) 268.

127 J. H. Fermor and A. Kjekshus, *Acta Chem. Scand.*, 22 (1968) 1628; 23 (1969) 1581.

128 S. Matsumoto, *Bull. Soc. Chem. Jap.*, 40 (1969) 2749.

129 A. M. Josepson and A. Z. Krist, *Naturwissenschaften*, A 24 (1969) 467.

130 L. M. Demidenko, N. N. Ustinzhanina and V. S. Bakunov, *Tr. Moskeekogo Teknol. Inst.*, (1969) 145.

131 N. P. Burmistrova and E. G. Volozkanina, *Zh. Fiz. Khim.*, 42 (1968) 2795.

132 L. G. Berg and N. P. Burmistrova, *Zh. Neorg. Khim.*, 5 (1960) 676.

133 M. Murrat and P. Barriac, *Bull. Soc. Chim. Fr.*, (1969) 2644.
134 A. Bergstein, *Collect. Czech. Chem. Commun.*, 20 (1955) 1058.
135 A. Bergstein, *Chem. Listy*, 50 (1956) 3.
136 A. Bergstein, *Collect. Czech. Chem. Commun.*, 21 (1956) 542.
137 R. F. S. Robertson and P. W. Selwood, *Rev. Sci. Instrum.*, 22 (1951) 146.
138 A. Michel, G. Chandron and J. Bénard, *Ferromagnetism and Antiferromagnetism, Colloques Internationaux*, Grenoble, 1950.
139 G. Chandron and J. Bénard, *Bull. Soc. Chim. Fr.*, (1949) 117.
140 L. J. E. Hofer, E. M. Cohn and W. C. Publes, *J. Amer. Chem. Soc.*, 71 (1949) 189.
141 J. E. Hofer, E. M. Cohn and W. C. Publes, *J. Phys. Colloid Chem.*, 53 (1949) 661.
142 J. M. Sturtevant, in A. Weissberger (editor), *Calorimetry in Techniques of Organic Chemistry*, 2nd Ed. Vol. I, Interscience, New York, 1949.
143 W. P. White, *J. Phys. Chem.*, 24 (1920) 393.
144 W. M. Smit, *Z. Elektrochem.*, 66 (1962) 779.
145 I. Proks, *Silikaty*, 14 (1970) 287.
146 J. J. Keavney and E. C. Eberlin, *J. Appl. Polym. Sci.*, 3 (1960) 47.
147 R. Perron, A. Mathieu and C. Paquot, *Bull. Soc. Chim. Fr.*, (1962) 2085.
148 C. Mazières, *Bull. Soc. Chim. Fr.*, (1961) 1695.
149 C. Mazières, *Anal. Chem.*, 36 (1964) 602.
150 A. Hrubý, *Czech. J. Phys.*, B22 (1972) 1187.
151 D. E. Etter, P. A. Tucker and L. J. Wittenberg, in R. F. Schwenker and P. D. Garn (editors), *Thermal Analysis*, Academic Press, New York, 1969, Vol. 2, p. 829.
152 J. Pöyhönen and K. Mansikka, *Phys. Kondens. Mater.*, 3 (1965) 218.
153 I. Proks and J. Zlatovský, *Chem. Zvesti*, 23 (1969) 620.
154 I. Proks, J. Zlatovsky and K. Adamkovičová, in H. G. Wiedemann (editor), *Thermal Analysis (Proc. IIIrd ICTA)*, Birkhäuser Verlag, Basel, 1972, Vol. 1, p. 461.
155 F. Ordway, *J. Res. Nat. Bur. Stand.*, 48 (1952) 152.
156 J. H. Flynn, in H. G. Wiedemann (editor), *Thermal Analysis (Proc. IIIrd ICTA)*, Birkhäuser Verlag, Basel, 1972, Vol. 1, p. 127.
157 J. H. Flynn, *Status of Thermal Analysis*, NBS Spec. Publ., O. Menis (editor) 338P119, Washington US Gov't. Print. Office. 1970.
158 M. Kubota and G. O. Spessart, *J. Phys. Chem.*, 70 (1966) 941.
159 S. M. Ellerstein, *J. Phys. Chem.*, 69 (1965) 2471.
160 E. M. Barrall, M. S. Porter and J. F Johnson, *J. Phys. Chem.*, 71 (1967) 895.
161 J. Jüntgen and K. H. van Heek, *Fortschritte der Chemischen Forschung*, 13, (3/4), Springer, 1970.
162 J. Šesták, P. D. Garn and R. F. Schwenker (editors), *Thermal Analysis*, Academic Press, New York, 1969, Vol. 2, p. 1085.
163 M. Meyer, M. Markowitz and D. A. Boryta, *J. Phys. Chem.*, 66 (1962) 1477.
164 A. Smith and R. P. Calvert, *J. Amer. Chem. Soc.*, 36 (1914) 1363.
165 *Thermal Analysis Newsletter*, Analytical Division, Perkin–Elmer Corp., Norwalk, Connecticut, No. 7.
166 M. Rigaud and T. R. Ingraham, *Can. Metalurg. Quart.*, 4 (1965) 237.
167 H. Schultze, *Glass* (F. Vieweg & Sohn, Braunschweig 1965) Verlag der Wissenschaften, Berlin 1969, p. 158.
168 E. L. Simmons and W. W. Wendlandt, *Thermochim. Acta*, 3 (1971) 25.
169 W. W. Wendlandt, personal communication, 1973.
170 A. Bergstein, *Reactivity of Solids*, Wiley, New York, 1969, p. 219.
171 A. Bergstein, J. Šesták, P. Holba, P. Kleinert and A. Funke, *Czech. J. Phys.*, B 17 (1967) 868.
172 F. Paulik, L. Erdey and S. Gál, *Z. Anal. Chem.*, 163 (1958) 321.
173 A. J. Majumdar, H. A. MacKinstry and R. Roy, *J. Phys. Chem. Solids*, 25 (1964) 1487.
174 J. Pöyhönen and K. Mansikka, *Phys. Kondens. Mater.*, 3 (1965) 218.
175 A. J. Majumdar and R. Roy, *J. Inorg. Nuclear Chem.*, 27 (1965) 1961.
176 K. K. Kelley, *U.S. Bur. Mines Bull.*, No. 393 (1936) 000.
177 N. L. Bowen, *Amer. J. Sci.*, 35 (1913) 577.
178 L. H. Adams and L. H. Cohen, *Amer. J. Sci.*, 264 (1966) 543.
179 G. P. Morie, T. A. Powers and C. A. Glover, *Thermochim. Acta*, 3 (1972) 259.
180 M. M. Markowitz and D. A. Boryta, *J. Phys. Chem.*, 66 (1962) 1477.

181 R. L. Stone, *Anal. Chem.*, 32 (1960) 1582.
182 B. G. Ellis and M. M. Mortland, *Amer. Mineral.*, 47 (1962) 371.
183 K. A. Buzdov, *Zh. Neorg. Khim.*, 11 (1966) 1251.
184 L. G. Berg and V. P. Kowyrzina, *Zh. Neorg. Khim.*, 9 (1964) 29.
185 J. N. Weber and R. Roy, *Amer. J. Sci.*, 263 (1965) 668.
186 L. G. Berg and K. P. Pribylov, *Zh. Neorg. Khim.*, 10 (1965) 1419.
187 I. S. Rassonskaja and O. S. Novikova, *Zh. Neorg. Khim.*, 11 (1966) 2041.
188 J. N. Weber, *Amer. Mineral.*, 51 (1966) 235.
189 E. Sturm, *Thermochim. Acta*, 4 (1972) 461.
190 V. V. Morarin and R. Mills, *Z. Phys. Chem.* (*Frankfurt am Main*), 78 (1972) 298.
191 J. Komrska, *Silikáty*, 11 (1967) 51.
192 N. H. Sze and G. T. Meaden, *Phys. Lett.*, 37A (1971) 393.
193 J. Akiyama, in H. G. Wiedemann (editor), *Thermal Analysis* (*Proc. IIIrd ICTA*), Vol. 1, Birkhäuser Verlag, Basel, 1972, p. 45.
194 B. Wunderlich, *Thermochim. Acta*, 5 (1973) 369.
195 E. M. Barrall II, *Thermochim. Acta*, 5 (1973) 377.